COMPTES RENDUS

(DOKLADY)

DE L'ACADÉMIE DES SCIENCES DE L'URSS

NOUVELLE SÉRIE

1943

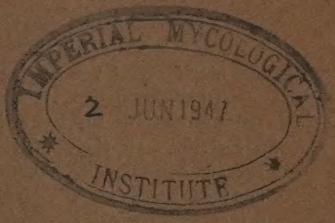

VOLUME XXXVIII

№ 2—3

ÉDITION DE L'ACADÉMIE DES SCIENCES DE L'URSS
MOSCOU

AVIS AUX AUTEURS

Les «Comptes Rendus (Doklady) de l'Académie des Sciences de l'URSS» paraissent tous les dix jours. Neuf numéros composent un volume pourvu d'une table des matières. Il y a quatre volumes par année.

Les «Comptes Rendus de l'Académie des Sciences de l'URSS» en de courtes communications précisent l'essentiel des travaux en préparation. Ces articles, ne dépassant pas en règle générale quatre pages, sont donnés en anglais ou en français. Ils embrassent les sciences mathématiques, physiques, naturelles et appliquées, mettant au jour les résultats de recherches scientifiques en cours ou qui viennent d'être achevées, et représentant ainsi les plus récentes données de l'investigation scientifique.

L'auteur a droit à 25 exemplaires de son article.

Adressez les manuscrits à la Rédaction des «Comptes Rendus», Kazan, rue Baumann, 19.

30 Janvier

COMPTES RENDUS

(DOKLADY)

DE L'ACADÉMIE DES SCIENCES DE L'URSS

COMITÉ DE RÉDACTION

A. Arbusov, de l'Académie, **A. Borissiak**, de l'Académie, **V. Chlopin**, de l'Académie, **A. Deborin**, de l'Académie, **A. Fersman**, de l'Académie, **A. Frumkin**, de l'Académie, **A. Kolmogoroff**, de l'Académie (vice rédacteur), **L. Orbeli**, de l'Académie (rédacteur en chef), **A. Richter**, de l'Académie, **S. Soboleff**, de l'Académie, **S. Wawilow**, de l'Académie (vice rédacteur)

NOUVELLE SÉRIE

11-me année

Paraissant tous les dix jours

1943

VOLUME XXXVIII, № 2—3

TABLE DES MATIÈRES

Pages

MATHÉMATIQUES

L. Lusternik. Ring of Intersections in a Certain Functional Space 59

V. Niemytzki. Intégration qualitative approximative du système d'équations $\frac{dx}{dt}=Q(x,y)$; $\frac{dy}{dt}=P(x,y)$ 62

MÉCANIQUE

E. L. Nicolai. Influence of Friction on Motion of Gyroscope with Cardan Suspension 66

ASTRONOMIE

B. J. Lèvin. Gas Evolution from the Nucleus of a Comet as Related to the Variations in its Absolute Brightness 72

N. N. Sytinskaya. Integral Photometry of the Solar Corona of September 21, 1941, in Different Parts of the Spectrum 75

PHYSIQUE

G. A. Grünberg. General Theory of the Focusing Action of Electrostatic and Magnetic Fields. III. Three-Dimensional (Twisted) Trajectories in the Presence of Both an Electrostatic and a Magnetic Field 78

PHYSIQUE APPLIQUÉE

V. A. Ostroumov and **V. N. Lepeshinskaya.** Piezoelectric Surgical Probe . . . 82

CHIMIE

A. M. Rubinstèin and **V. G. Kuznètzov.** X-ray Analysis of a New Type of Complex Compounds of Tetravalent Platinum 85

CHIMIE DU GLOBE

B. N. Melentiev. A Rapid Method for Determining Al_2O_3 in a Nepheline Concentrate 93

PHYSIOLOGIE DES PLANTES

A. A. Smolin. Experimental Elimination of Dormancy in Tau-Saghyz 96

PATHOLOGIE GÉNÉRALE

S. P. Alfeeva. Experimental Spring-Summer Tick Encephalitis in Birds 99

PARASITOLOGIE

N. Gruzdeva. Length of Survival Under Water of Various Stages and Species of Ticks, Transmitters of Parasitic Encephalitis in the Maritime Province, Far East of the USSR 102

Édition de l'Académie des Sciences de l'URSS

Moscou 1943

Comptes Rendus (Doklady) de l'Académie des Sciences de l'URSS
1943. Volume XXXVIII, № 2—3

MATHEMATICS

RING OF INTERSECTIONS IN A CERTAIN FUNCTIONAL SPACE

By L. LUSTERNIK

(Communicated by S. L. Soboleff, Member of the Academy, 1.X.1942)

In one of my earlier papers I have investigated by geometrical methods some topological properties of the space of admissible curves for the simplest variational problem that are connected with the questions of intersection ([1],[2]). In the present work I am investigating these questions in an analogous space by means of more general methods that are applicable to the other functional spaces and obtain more complete results. It is worth noticing that the classes of functional spaces, which are most important for the analysis, namely those of locally bicompact spaces and of the spaces of similar structure, constitute a quite natural domain of application of the combinatorial topological theory of locally bicompact spaces developed by P. Alexandroff ([3],[4]).

Definitions. The l-dimensional Euclidean sphere in the $(l+1)$-dimensional Euclidean space will be denoted by S_l. Let a and b be any two points on S_l; $R(S_l; a, b; N)$ denotes then the totality of rectifiable curves on S_l joining the points a and b, the length of which does not exceed N. The totality of all rectifiable curves on S_l joining a and b is denoted by $R(S_l; a, b)$. $R(S_l; a, b) = \sum_N R(S_l; a, b; N)$, where N ranges through a sequence tending to $+\infty$. The distance $\rho(q, q_1)$ between any two curves belonging to $R(S_l; a, b)$ will be understood in the sense of Frechet. Under this assumption $R(S_l; a, b; N)$ becomes a compactum.

In the well known book by M. Morse ([5]) lower homologies modulo 2 in $R(S_l; a, b)$ are investigated. The results of our papers referred to above correspond to the intersections in these spaces also modulo 2. We now intend to investigate lower and upper homologies in Alexander-Kolmogoroff sense and the ring of intersections in these spaces, as well as some questions relating to the homotopy. The methods applied here can be used for the study of other non-linear functional spaces.

For the sake of simplicity consider the case $l=2$, and let $R=R(S_2; a, b)$, $R_N=R(S_2; a, b; N)$. Denote by Z_c the totality of all curves belonging to R passing through the point c different from a and b. In general, if $c_1, c_2, \ldots, c_n$ are points different from a and b, $Z_{c_1, c_2, \ldots, c_n}$ denotes the totality of all curves belonging to R and passing through $c_1, c_2, \ldots c_n$ in the prescribed order in the direction from a to b.

We shall construct the upper n-dimensional cycles $\overline{Z}_{c_1, c_2, \ldots, c_n}$ corresponding geometrically to the sets $Z_{c_1, c_2, \ldots, c_n}$.

Take $\varepsilon > 0$ and a point c on S_2, whose distances from a and b exceed ε. Consider the curves q_1 and q_2 such that their lengths do not exceed $\frac{1}{10\varepsilon}$ and

the distance between them is less than or equal to ε. The curves q_1 and q_2 are continuous images of the segment [0,1]: to every value of the parameter t, $0 \leqslant t \leqslant 1$, there correspond a point a_t^1 on q_1 and a point a_t^2 on q_2. In particular, $a_0^1 = a_0^2 = a$, $a_1^1 = a_1^2 = b$. According to Frechet's definition of the distance between the curves q_1 and q_2, the latter can be parametrized in such a way that the distances between the points a_t^1 and a_t^2, corresponding to one and the same value of t, do not exceed ε. We choose such parametrizations and join the pairs of points a_t^1 and a_t^2 (at the same t) by geodesics (whose lengths are evidently less than or equal to ε). Denote by Q_{01} the surface drawn on the closed curve $q_1 - q_2$ formed by the geodesics a_t^1, a_t^2, when t ranges through the segment [0,1]. The part of this surface formed by the geodesics that correspond to the values of t, belonging to the segment $[t_1, t_2] \subset [0,1]$, will be denoted by $Q_{t_1 t_2}$. Denote further by $\psi_{01}^{\varepsilon}(q_1, q_2; c)$ the number of times that c is covered by Q_{01}. It is possible to show that the values of this function do not depend on the parametric representation of q_1 and q_2 satisfying the above condition (that the distance between all the corresponding points do not exceed ε). In general, by $\psi_{t_1 t_2}^{\varepsilon}(q_1, q_2; c)$ we mean the number of times that the point c is covered by $Q_{t_1 t_2}$. The sequence of functions $f_k^1 = \psi_{01}^{\varepsilon_k}(q_1, q_2; c)$ with ε_k approaching zero at $k \to \infty$ determines a one-dimensional cycle $\overline{Z}_c$.

We now shall define the functions $\psi_{t_1 t_2}^{\varepsilon}(q_1, q_2, \ldots, q_{n+1}, c_1, c_2, \ldots, c_n)$ of $n+1$ curves for any n recurrently. We choose n points $c_1, c_2, \ldots, c_n$ on S_2, whose distances from a and b and one from another exceed ε. The distances between any two of the curves $q_1, q_2, \ldots q_{n+1}$ are supposed to be less than or equal to ε and the lengths of the curves not to exceed $\frac{1}{10\varepsilon}$.

The functions $\psi_{t_1 t_2}^{\varepsilon}(q_i, q_j, c_l)$ are already defined. Suppose that $\psi_{t_1 t_2}^{\varepsilon}(q_{i_1}, q_{i_2}, \ldots, \ldots, q_{i_m}, q_{i_{m+1}}, c_{j_1}, c_{j_2}, \ldots, c_{j_m})$ are defined for $m < n$. We then put

$$\psi_{t_1 t_2}^{\varepsilon}(q_1, q_2, \ldots, q_{n+1}, c_1, c_2, \ldots, c_n) =$$

$$= \int_{t=t_1}^{t_2} \psi_{tt_2}^{\varepsilon}(q_2, q_3, \ldots, q_{n+1}, c_2, c_3, \ldots, c_n)\, d\psi_{tt_2}^{\varepsilon}(q_1, q_2, c_1).$$

Let us choose now an everywhere dense net $q^1, q^2, q^3, \ldots$ on R and define a sequence of functions f_k^n depending on $n+1$ curves as follows: let the sequence $\varepsilon_k > 0$ tend to zero at $k \to \infty$. If the curves $q^{\alpha_1}, q^{\alpha_2}, \ldots, q^{\alpha_{n+1}}$ with the indices written in their natural order belong to the net, the distances between any two of these curves are less than or equal to ε and their lengths do not exceed $\frac{1}{10\varepsilon}$, then

$$f_k^n(q^{\alpha_1}, q^{\alpha_2}, \ldots, q^{\alpha_{n+1}}) = \psi_{01}^{\varepsilon_k}(q^{\alpha_1}, q^{\alpha_2}, \ldots, q^{\alpha_{n+1}}; c_1, c_2, \ldots, c_n).$$

Assume now that every even permutation of curves leaves the values of f_k^n invariant, while every odd permutation alters the sign of f_k^n. The functions f_k^n are thus defined for all aggregates of $n+1$ curves belonging to the everywhere dense net with their mutual distances $\leqslant \varepsilon$ and the lengths $\leqslant \frac{1}{10\varepsilon}$. By means of a passage to the limit we define f_k^n for all aggregates of curves belonging to R and satisfying the same conditions imposed on their distances and lengths.

The sequence of functions f_k^n $(k \to \infty)$ thus defined determines an n-dimensional ∇-cycle that we denote by $\overline{Z}_{c_1 c_2 \ldots c_n}$. Exactly as in the case of the Alexander product, it is possible to prove that up to ∇-homologies this cycle does not depend on the numeration of the everywhere dense net.

Remark 1. Consider the set T_{ε_k} of those curves q that belong to at least one aggregate of curves $q, q_2, q_3 \ldots, q_{n+1}$ for which $f_k^n(q, q_2, \ldots, q_{n+1}) \neq 0$. The set $Z_{c_1c_2\ldots c_n}$ defined above is the topological limit of sets T_{ε_k} at $k \to \infty$. Thus, we may say that $Z_{c_1c_2\ldots c_n}$ is the «carrier» of the cycle $\bar{Z}_{c_1c_2\ldots c_n}$.

Remark 2. Two n-dimensional cycles U_1 and U_2 will be called ∇-homologous in R, if the cycles $U_1 \times R_N$ and $U_2 \times R_N$ are ∇-homologous in R_N, whenever N is sufficiently large.

By the definition of the cycles $\bar{Z}_{c_1c_2\ldots c_n}$ and the properties of the Alexander product we can obtain:

$$\bar{Z}_{c_1c_2\ldots c_n} \times \bar{Z}_{d_1d_2\ldots d_m} = \sum \pm \bar{Z}_{e_1e_2\ldots e_{n+m}}, \tag{1}$$

where $e_1, e_2, \ldots, e_{n+m}$ is a permutation of elements $c_1, c_2, \ldots, c_n, d_1, d_2, \ldots, d_m$ such that the elements $c_i (i = 1, 2, \ldots, n)$ as well as the elements $d_j (j = 1, 2, \ldots, m)$ are written down in the natural order of their indices (for instance, if we have c_1, c_2, d_1, d_2, we may take 6 permutations as follows: c_1, c_2, d_1, d_2; c_1, d_1, c_2, d_2; d_1, c_1, c_2, d_2; d_1, c_1, c_2, d_2; d_1, c_1, d_2, c_2; d_1, d_2, c_1, c_2). As to the sign of a summand in (1), it will be determined by that of $(-1)^{\sum_i r_i}$, where r_i is the number of elements $d_1, d_2, \ldots, d_m$ preceding c_i in the corresponding permutation. The summation in (1) is to be extended over all such permutations. All cycles $Z_{g_1g_2\ldots g_e}$, corresponding to different aggregates of points $g_1, g_2 \ldots, g_e$, are ∇-homologous to one another, and, in particular, the cycles on the right-hand side of (1) are ∇-homologous to one another. Consequently, denoting by $\bar{Z}_n$ the homology class of the cycles $\bar{Z}_{g_1g_2\ldots g_n}$, we shall have

$$\bar{Z}_n \times \bar{Z}_m = C_n^m \bar{Z}_{n+m}, \tag{2}$$

where $C_n^m = \sum (-1)^{\sum_i r_i}$, the sum being extended over all permutations defined above; the exponent $\sum_i r_i$ is already defined.

One can prove that if m and n are odd, $C_m^n = 0$, and thus $\bar{Z}_m \times \bar{Z}_n \tilde{\nabla} 0$. In particular, $\bar{Z}_1 \times \bar{Z}_1 \tilde{\nabla} 0$. At the same time $C_1^{2k} \neq 0$.

A calculation gives $C_2^n \neq 0$. Consequently, if the homologies are taken with respect to a sufficiently large modulus, then

$$\bar{Z}_2 \times \bar{Z}_n = C_2^n \bar{Z}_{n+2} \tilde{\nabla} 0.$$

Under the same condition

$$\underbrace{\bar{Z}_2 \times \bar{Z}_2 \times \ldots \times \bar{Z}_2}_{n \text{ times}} = C_{2n} \bar{Z}_{2n} \tilde{\nabla} 0, \tag{3}$$

where $C_{2n} = C_2^2 C_4^2 \ldots C_{2n-2}^2$ and

$$\bar{Z}_1 \times \underbrace{\bar{Z}_2 \times \bar{Z}_2 \times \ldots \times \bar{Z}_2}_{n \text{ times}} = C_{2n+1} \bar{Z}_{2n+1} \tilde{\nabla} 0, \tag{4}$$

where $C_{2n+1} = C_1^{2n} C^n$.

Stekloff Mathematical Institute.
Academy of Sciences of the USSR.

Received
1. X. 1942.

REFERENCES

[1] L. Lusternik, C. R. Acad. Sci. URSS, XXVII, No. 8 (1940). [2] L. Lusternik, ibid., XXVII, No. 8 (1940). [3] P. Alexandroff, Annals of Math., 30, 101—187 (1929), [4] P. Alexandroff, Trans. Amer. Math. Soc., 49, 41—105 (1941). [5] M. Morse, The Calculus of Variations in the Large (1934).

Comptes Rendus (Doklady) de l'Académie des Sciences de l'URSS
1943. Volume XXXVIII, № 2—3

MATHÉMATIQUES

INTÉGRATION QUALITATIVE APPROXIMATIVE DU SYSTÈME D'ÉQUATIONS $\frac{dx}{dt}=Q(x,y)$, $\frac{dy}{dt}=P(x,y)$

Par V. NIEMYTZKI

(Présenté par A. N. Kolmogoroff, de l'Académie, le 8.X. 1942)

1. Considérons le système d'équations

$$\frac{dx}{dt}=Q(x,y);\quad \frac{dy}{dt}=P(x,y) \tag{1}$$

en supposant que les fonctions $Q(x,y)$ et $P(x,y)$ sont définies et continues dans un certain domaine G et les dérivées partielles $\frac{\partial P}{\partial x}$, $\frac{\partial P}{\partial y}$, $\frac{\partial Q}{\partial x}$, $\frac{\partial Q}{\partial y}$ sont bornées dans chaque domaine borné appartenant à G.

Si le domaine $\Gamma\subset G$ ne contient pas de points singuliers, on peut considérer au lieu du système (1) le système (1′):

$$\frac{dx}{d\tau}=\frac{Q}{\sqrt{P^2+Q^2}},\qquad \frac{dy}{d\tau}=\frac{P}{\sqrt{P^2+Q^2}} \tag{1′}$$

$$\frac{d\tau}{dt}=\sqrt{P^2+Q^2}>0. \tag{2}$$

Il suit de la condition (2) que dans le domaine Γ non seulement les courbes intégrales de (1) et (1′) coïncident, mais les tableaux dynamiques (l'ensemble de points α- et ω-limites) sont identiques.

Définition 1. *Un système de fonctions* $x=\bar{x}(\tau)$, $y=\bar{y}(\tau)$ *est nommé* ε-*solution du système* (1) *et* (1′), *si les conditions suivantes sont vérifiées:* 1) $\bar{x}(\tau)$ *et* $\bar{y}(\tau)$ *possèdent les dérivées continues pour* $t_0\leqslant t\leqslant t_1$, *sauf peut-être en un nombre fini de points où elles possèdent des dérivées droites et gauches continues;* 2) *les dérivées droites et gauches pour chaque valeur de* τ $(\tau_0\leqslant\tau\leqslant\tau_1)$ *vérifient le système* (1′) *à* ε *près, c'est-à-dire*

$$D_+\bar{x}(\tau)=\frac{Q(\bar{x},\bar{y})}{\sqrt{P^2(\bar{x},\bar{y})+Q^2(\bar{x},\bar{y})}}=\omega_1(\bar{x},\bar{y})$$

où $|\omega_1(\bar{x},\bar{y})|<\varepsilon$ *et de même pour* $D_-\bar{x}(\tau)$, $D_+\bar{y}(\tau)$, $D_-\bar{y}(\tau)$; 3) *la courbe* $x=\bar{x}(\tau)$, $y=\bar{y}(\tau)$ *n'a pas de points multiples pour* $\tau_0\leqslant\tau\leqslant\tau_1$.

La définition des ε-solutions et une méthode pour les trouver en construisant les lignes polygonales d'Euler ont été données par M. Ch. de la Vallée-Poussin.

2. Soit Γ un domaine connexe qui ne contient pas de points isolés ni à l'intérieur, ni sur la frontière et soit Γ_0 un domaine connexe tel que $\bar{\Gamma}_0\subset\Gamma$ et la distance de Γ_0 à la frontière de Γ est égale à $\Delta>0$.

Définition 2. *On appelle vitesse moyenne (ou bien vitesse à* ε *près) de la variation du champ dans* $\bar{\Gamma}_0$ *la borne supérieure des nombres* η *tels que si* $\rho(A,B)<\eta$, *où le segment* AB *appartient à* $\bar{\Gamma}_0$, *alors l'angle entre les vecteurs du champ défini par* (1) *aux points* A *et* B *est inférieur ou égal à* ε.

Désignons la vitesse moyenne par v_ε. Dans la suite nous aurons à considérer le nombre $\eta_\varepsilon(\bar{\Gamma}) = \inf(\varepsilon, v_\varepsilon)$.

Définition fondamentale 3. *Soit $F = \{L(\tau)\}$ une famille d'arcs de courbes intégrales situées dans Γ_0. Nous dirons qu'un nombre fini de lignes polygonales $\Lambda_1, \Lambda_2, \ldots, \Lambda_k$ se trouvant dans la sphère $S\left(\Gamma_0, \frac{\Delta}{3}\right)$ forme un ε-réseau sur la famille F, si les conditions suivantes sont vérifiées:*

1) *chaque ligne polygonale est une ε-solution;*

2) *quel que soit l'arc L de la famille donnée, il existe une ligne polygonale Λ_i telle que l'écart $\alpha(L, \Lambda_i) \leqslant \eta_\varepsilon(\bar{\Gamma})$.*

3) *Quelle que soit la ligne polygonale Λ_i, il existe un arc L d'une courbe intégrale du système (1) (qui peut ne pas appartenir à F) tel que*

$$\alpha(L, \Lambda_i) \leqslant \eta_\varepsilon(\bar{\Gamma}).$$

Un ε-réseau construit sur une famille donnée de courbes intégrales donne un tableau approximatif qualitatif de l'allure des courbes intégrales formant cette famille.

3. Soit E_x l'ensemble des points d'une ε-solution, où l'on a: ou bien $\frac{d\bar{x}}{d\tau} = 0$, ou bien $D_+\bar{x}(\tau)$ et $D_-\bar{x}(\tau)$ sont de signes opposés, et E_y — l'ensemble de points d'une ε-solution, où l'on a: ou bien $\frac{d\bar{y}}{d\tau} = 0$, ou bien $D_+\bar{y}(\tau)$ et $D_-\bar{y}(\tau)$ sont de signes opposés.

Définition 4. *Si un arc $\overset{\frown}{AB}$ d'une ε-solution contient simultanément des points de l'ensemble E_x et de l'ensemble E_y, nous dirons que les points A et B sont situés sur deux segments essentiellement différents de cette ε-solution.*

Soit $\widehat{AB}$ une ε-solution non fermée.

Définition fondamentale 5. *Appelons indice d'une ε-solution $\widehat{AB}$ la borne inférieure des distances des points C et D appartenant à $\widehat{AB}$ et situés sur deux segments essentiellement différents; s'il n'existe pas de points C et D situés sur deux segments essentiellement différents, on prend pour l'indice de $\widehat{AB}$ la distance entre ses points extrêmes.*

4. Théorème 1. *Soit donné un système $\frac{dx}{dt} = Q(x, y)$, $\frac{dy}{dt} = P(x, y)$ et un domaine Γ_0, précédemment défini; si les nombres $\varepsilon < \frac{\pi}{42}$ et n sont donnés, on peut indiquer une méthode qui permet de construire un ε-réseau sur la famille F des courbes intégrales situées dans Γ_0 et dont l'indice est supérieur ou égal à $\frac{1}{n}$; d'ailleurs, à cet effet il suffit de faire un nombre fini d'opérations arithmétiques et ce nombre ne dépend que de ε et n.*

Ce procédé consiste en ce qu'on construit un nombre suffisant de lignes polygonales d'Euler, et le but du théorème est d'indiquer nombre de ces lignes et de leurs segments en fonction de ε et n. La possibilité d'indiquer un tel nombre est fondée sur les lemmes suivants:

Lemme 1. *Chaque ε-solution $\left(\varepsilon < \frac{\pi}{42}\right)$ située dans Γ_0 et d'indice α possède une longueur S_L qui vérifie l'inégalité*

$$S_L \leqslant 2\,\frac{\mathrm{mes}^2 S(\bar{\Gamma}_0, \rho_0)}{\rho_0^3}, \quad \text{où} \quad \rho_0 = \inf\left(\alpha, \eta_{\frac{\pi}{42}}(\bar{\Gamma}_0)\right).$$

Lemme 2. *Soient $x = \bar{x}(\tau)$, $\bar{y} = y(\tau)$ et $x = \bar{\bar{x}}(\tau)$, $y = \bar{\bar{y}}(\tau)$ deux ε-solutions situées dans Γ_0; alors sur le segment $0 \leqslant \tau \leqslant S$ on a les inégalités*

$$\max\ \bar{x} - \bar{\bar{x}} | \leqslant 4^4 F_{\bar{\Gamma}_0}(S+1)\left(d + \frac{8F_{\bar{\Gamma}_0} + 2S}{F_{\bar{\Gamma}_0}}\varepsilon\right)$$

et de même pour $\max|\bar{y}-\bar{\bar{y}}|$, *où*

$$F_{\bar{\Gamma}_0}=\sup\left\{\frac{\partial P}{\partial x},\ \frac{\partial P}{\partial y},\ \frac{\partial Q}{\partial x},\ \frac{\partial Q}{\partial y}\right\}\quad \textit{dans } \Gamma_0 \textit{ et}$$

$$d=\sup\{|\bar{x}(0)-\bar{\bar{x}}(0)|,\ |\bar{y}(0)-\bar{\bar{y}}(0)|\}.$$

Remarquons qu'en nous appuyant sur ces lemmes pour trouver le nombre des lignes polygonales nécessaires et le nombre de leurs segments nous n'employons pas, en réalité, les indices, mais la longueur maximale possible des courbes intégrales.

5. Considérons deux suites

$$\varepsilon_1,\ \varepsilon_2,\ \varepsilon_3,\ \ldots,\ \varepsilon_k\ \ldots\longrightarrow 0$$
$$1,\ \frac{1}{2},\ \frac{1}{3},\ \ldots,\ \frac{1}{k}\ \ldots,\longrightarrow 0.$$

Appelons n-ième pas du procédé d'intégration qualitative la construction d'un ε_n-réseau sur la famille des courbes intégrales d'indice supérieur ou égal à $\frac{1}{n}$ et situées dans Γ_0.

Définition 6. *Supposons que la limite topologique de la suite des droites* $L_1, L_2, \ldots, L_n, \ldots$ *est un certain arc* L. *Nous dirons que les coefficients angulaires des lignes polygonales convergent vers les coefficients angulaires de l'arc* L *si, quel que soit le point* A *sur* L *et quelle que soit la suite des points* $A_1, A_2, \ldots, A_n, \ldots$ *convergeant vers* A *et tels que* $A_n \subset L_n$, *les cosinus directeurs des tangentes (droites et gauches) aux lignes polygonales* L_n *aux points* A_n *convergent vers les cosinus directeurs de la tangente à* L *au point* A.

Soit k un entier quelconque et soient

$$\Lambda_1^{(1)},\ \Lambda_2^{(1)},\ \ldots,\ \Lambda_{n_1}^{(1)},\ \Lambda_{n_1+1}^{(2)},\ \Lambda_{n_1+2}^{(2)},\ \ldots,\ \Lambda_{n_2}^{(2)},\ \ldots,\Lambda_{n_k+1}^{(k)},\ \Lambda_{n_k+2}^{(k)},\ \ldots,\ \Lambda_{n_{k+1}}^{(k)},\ \ldots$$

les lignes polygonales construites dans les k premiers pas du procédé d'intégration qualitative; appelons ces lignes polygonales des polygonales approximatives.

Théorème 2. *Quel que soit l'arc intégral fini* L *situé dans* Γ_0, *on peut indiquer une suite de lignes polygonales approximatives dont* L *est la limite topologique et dont les coefficients angulaires convergent vers les coefficients angulaires de* L. *Inversement, étant donnée une suite infinie de polygonales approximatives* $\Lambda_1, \Lambda_2, \ldots \Lambda_n, \ldots$ *telles que* $\sum_{n=1}^{\infty} \Lambda_n \subset \Gamma_0$, *si cette suite converge vers un certain continu* L *et les longueurs des lignes polygonales tendent vers une limite finie, alors* L *est une courbe intégrale appartenant à* Γ_0.

6. Ces considérations permettent d'indiquer une méthode effective pour la recherche des solutions périodiques et, en particulier, des cycles limites.

Tout d'abord énonçons une proposition dont la méthode de la démonstration sera indiquée dans une Note suivante («Intégration qualitative du système d'équations $\frac{dx}{dt}=Q(x,y)$, $\frac{dy}{dt}=P(x,y)$ en première approximation»).

Soit ρ_0 un certain nombre et E l'ensemble de points du plan R que l'on exclut par une raison quelconque, les points singuliers y compris; soit $\bar{E}=F$. Décrivons autour de F une sphère de rayon ρ_0; soit $\hat{\Gamma}_{\rho_0}=R-\bar{S}(F,\rho_0)$. Définissons pour $\hat{\Gamma}_{\rho_0}$ le nombre $\eta_{\frac{\pi}{12}}(\hat{\Gamma}_{\rho_0})$. Soit ensuite

$$\bar{\rho}=\min\left\{2\rho_0,\ \rho_0+\frac{\pi}{12\sqrt{3}}\eta_{\frac{\pi}{12}}(\hat{\Gamma}_{\rho_0})\right\}$$

et soit enfin

$$\Gamma_{\rho_0}=R-S(F,\bar{\rho}).$$

Le domaine Γ_{ε_0} sera nommé domaine canonique. Il est évident que chaque domaine contenu avec sa frontière dans $R-F$ peut être enfermé en un certaine domaine canonique.

Définition 7. *Appelons indice d'une ε-solution fermée L la borne inférieure des distances des points C et D appartenant à L et tels que sur les deux arcs joignant ces deux points suivant L ils sont situés sur deux segments essentiellement différents.*

Théorème 3. *Dans un domaine canonique Γ il ne peut exister de courbes fermées d'indice inférieur ou égal à* $\frac{1}{\sqrt{3}}\eta_{\frac{\pi}{12}}(\Gamma)$.

En vertu du lemme 1 il est facile d'en déduire que *toutes les solutions périodiques situées dans Γ ont une longueur qui ne surpasse pas un certain nombre S.*

Cela posé, effectuons la construction suivante. Soit $\varepsilon_0 < 1$ arbitraire; construisons en vertu de la remarque du théorème 1 un ε_0-réseau sur la famille des arcs intégrals contenus dans Γ et de longueur $\leqslant S$. Choisissons parmi les lignes polygonales approximatives celles dont les extrémités se trouvent à distance inférieure ou égale à $2\eta_{\varepsilon_0}(\Gamma)$.

Soient $\Lambda_1^0, \Lambda_2^0, \ldots, \Lambda_{s_0}^0$ ces lignes polygonales. Prenons maintenant la suite $\varepsilon_1 = \frac{\varepsilon_0}{2}, \ldots, \varepsilon_k = \frac{\varepsilon_0}{2^k}, \ldots \to 0$. Construisons un ε_1-réseau sur la même famille et choisissons parmi les lignes polygonales approximatives celles dont les extrémités se trouvent à distance inférieure ou égale à $2\eta_{\varepsilon_1}$, et dont l'écart de l'une des lignes Λ_i^0 ne surpasse pas $\eta_{\varepsilon_0}+\eta_{\varepsilon_1}$. Les lignes polygonales construites au second pas du procédé et dont l'écart d'une certaine Λ_i^0 est inférieur ou égal à $\eta_{\varepsilon_0}+\eta_{\varepsilon_1}$ seront désignées par $\Lambda_{i_1}, \Lambda_{i_2}, \ldots \Lambda_{i s_1}$; nous dirons qu'elles sont subordonnées à Λ_i. Passons au troisième pas du procédé. Construisons un ε_2-réseau, choisissons les lignes polygonales, dont les extrémités se trouvent à distance inférieure ou égale à $2\eta_{\varepsilon_2}$ et qui vérifient simultanément les inégalités

$$\alpha(L_p^{(3)}, \Lambda_i^0) \leqslant \eta_{\varepsilon_0}+\eta_{\varepsilon_1}, \quad \alpha(L_p^{(3)}, \Delta_{ij}) \leqslant \eta_{\varepsilon_1}+\eta_{\varepsilon_2}.$$

Parmi les lignes polygonales choisies celles qui vérifient la seconde des deux inégalités précédentes pour i et j fixes seront nommées subordonnées à Λ_{ij} et désignées par Λ_{ijk}, et ainsi de suite. On prolongera ce procédé ou bien jusqu'à ce qu'on ne trouve plus de lignes polygonales vérifiant les conditions indiquées, ou bien indéfiniment.

Comme résultat on obtient un A-tableau

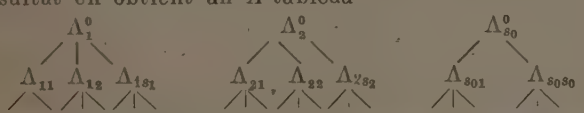

Théorème 4. 1) *Quelle que soit la solution L fermée située dans Γ, il existe une suite de lignes polygonales subordonnées les unes aux autres, contenues dans le A-tableau précédemment construit et telles que L est leur limite topologique et leurs coefficients angulaires convergent vers les coefficients angulaires de L.* 2) *Chaque suite infinie de lignes polygonales subordonnées les unes aux autres converge vers une certaine solution périodique au sens de la limite topologique ainsi qu'au sens de la convergence des coefficients angulaires.*

Ce théorème donne un procédé régulier pour la recherche des solutions périodiques; dans le cas où les solutions périodiques n'existent pas, le procédé permet de reconnaître leur absence après un nombre fini de pas, et inversement, si le procédé peut être prolongé indéfiniment, il démontre l'existence des solutions périodiques. Ainsi on a une analogie complète entre l'étude de l'existence des cycles limites et le problème de distinguer les centres et les foyers.

Institut Mathématique.
Université d'État. Moscou.

Manuscrit reçu
le 20.VIII.1942.

Comptes Rendus (Doklady) de l'Académie des Sciences de l'URSS
1943. Volume XXXVIII, № 2—3

MECHANICS

INFLUENCE OF FRICTION ON MOTION OF GYROSCOPE WITH CARDAN SUSPENSION

By E. L. NICOLAI

(Communicated by A. F. Joffe, Member of the Academy, 14.IX.1942)

§ 1. Image-point Method

The case considered here is a pseudo-regular precessional motion of a gyroscope rotating at high speed in a cardan suspension under the action of constant external moments M_1 and M_2 (about the axes of rotation of the inner and outer rings of the suspension, respectively). Allowance is also made for the moment of friction L_1 and L_2 on the axes of the suspension rings.

The motion of this gyroscope is expressed with reasonable approximation by the differential equations

$$\left.\begin{aligned} A_0\ddot{\beta} - C\omega\dot{\alpha}\cos\beta_0 &= -(M_1+L_1) \\ B_0\ddot{\alpha} + C\omega\dot{\beta}\cos\beta_0 &= M_2+L_2 \end{aligned}\right\} \qquad (1)$$

Here α and β are the angles of rotation of the outer and inner suspension ring, respectively*; β_0 is the initial value of the angle β; ω is a constant great angular velocity of the proper motion of the gyroscope; C is the polar moment of inertia of the gyroscope; the constants A_0 and B_0 assume the values

$$A_0 = A + A_1, \quad B_0 = (A + C_1)\cos^2\beta_0 + A_1\sin^2\beta_0 + A_2,$$

where A is the equatorial moment of inertia of the gyroscope; A_1 and C_1 are the equatorial and polar moments of inertia of the inner ring, respectively; A_2 is the moment of inertia of the outer ring with respect to its axis of rotation.

Concerning the moments of friction L_1 and L_2, the following assumptions are adopted:

$$\left.\begin{aligned} L_1 &= K_1, && \text{if } \dot{\beta} > 0; & L_2 &= -K_2, && \text{if } \dot{\alpha} > 0 \\ L_1 &= -K_1, && \text{if } \dot{\beta} < 0; & L_2 &= K_2, && \text{if } \dot{\alpha} < 0 \\ -K_{10} < L_1 &< K_{10} && \text{if } \dot{\beta} = 0; & -K_{20} < L_2 &< K_{20}, && \text{if } \dot{\alpha} = 0 \end{aligned}\right\} \qquad (2)$$

---

* These angles are supposed to be measured in the way adopted in the author's text book «Theoretical Mechanics»(1).

Here K_1, K_2, K_{10} and K_{20} are positive constants ($K_{10} > K_1$, $K_{20} > K_2$). The sign of the moment L_1 is determined on the consideration that a positive change of angle β corresponds to a rotation of the inner ring in the negative direction.

Equations (1) are valid within a limited interval of time during which angle β remains near enough to its inital value β_0. In the sequel it is supposed that the motion under consideration does not go beyond such an interval.

Let us introduce new variables x and y by putting

$$x = \alpha\sqrt{B_0}, \quad y = \beta\sqrt{A_0}, \tag{3}$$

and denote

$$\left.\begin{aligned} k_1 &= \frac{M_1}{\lambda\sqrt{A_0}}, \quad k_2 = \frac{M_2}{\lambda\sqrt{B_0}}, \quad m = \frac{L_1}{\lambda\sqrt{A_0}}, \quad n = \frac{L_2}{\lambda\sqrt{B_0}} \\ a &= \frac{K_1}{\lambda\sqrt{A_0}}, \quad b = \frac{K_2}{\lambda\sqrt{B_0}}, \quad a_0 = \frac{K_{10}}{\lambda\sqrt{A_0}}, \quad b_0 = \frac{K_{20}}{\lambda\sqrt{B_0}}, \\ \lambda &= \frac{C\omega\cos\beta_0}{\sqrt{A_0 B_0}} \end{aligned}\right\} \tag{4}$$

With these denotations equations (1) take the form

$$\left.\begin{aligned} \ddot{x} + \lambda\dot{y} &= \lambda(k_2 + n) \\ \ddot{y} - \lambda\dot{x} &= -\lambda(k_1 + m) \end{aligned}\right\} \tag{5}$$

and conditions (2) read thus

$$\left.\begin{aligned} m = a, &\quad \text{if } \dot{y} > 0, \qquad n = -b, \quad \text{if } \dot{x} > 0 \\ m = -a, &\quad \text{if } \dot{y} < 0; \qquad n = b, \quad \text{if } \dot{x} < 0 \\ -a_0 < m < a_0, &\quad \text{if } \dot{y} = 0; \qquad -b_0 < n < b_0, \quad \text{if } \dot{x} = 0 \end{aligned}\right\} \tag{6}$$

Integration of equations (5) over a period of time during which $\dot{x}$ and $\dot{y}$ are not zero and do not change their signs, gives

$$\left.\begin{aligned} \dot{x} - k_1 - m &= (\dot{x}_0 - k_1 - m)\cos\lambda t - (\dot{y}_0 - k_2 - n)\sin\lambda t \\ \dot{y} - k_2 - n &= (\dot{x}_0 - k_1 - m)\sin\lambda t + (\dot{y}_0 - k_2 - n)\cos\lambda t \end{aligned}\right\} \tag{7}$$

$$\left.\begin{aligned} \lambda(x - x_0) &= \dot{y} - \dot{y}_0 + (k_1 + m)\lambda t, \\ \lambda(y - y_0) &= -(x - x_0) + (k_2 + n)\lambda t, \end{aligned}\right\} \tag{8}$$

where $\dot{x}_0$, $\dot{y}_0$, x_0, y_0 are initial values of $\dot{x}$, $\dot{y}$, x, y. Equations (7) can be reduced to the form

$$\left.\begin{aligned} \dot{x} - k_1 - m &= r\cos(\lambda t + \varphi), \\ \dot{y} - k_2 - n &= r\sin(\lambda t + \varphi), \end{aligned}\right\} \tag{9}$$

where r and φ are constants.

Now consider point $P(\dot{x}, \dot{y})$. Its movement in the plane $\dot{x}$, $\dot{y}$ gives an image of the variations of $\dot{x}$ and $\dot{y}$. We assign to this point the name of «image-point».

From equations (9) it is seen that within an interval of time during which $\dot{x}$ and $\dot{y}$ are not zero and suffer no alteration of sign, the image-point P moves in the plane $\dot{x}$, $\dot{y}$ describing an arc of circle having its centre at point $A(k_1 + m, k_2 + n)$ and this movement is in the positive direction at a constant angular velocity λ.

Remembering condition (6), we conclude that to each quadrant of the plane $\dot{x}$, $\dot{y}$ belongs its particular centre of rotation A. In the annexed table the four rotation centres A_1, A_2, A_3 and A_4 are referred to the respective quadrants of the plane $\dot{x}$, $\dot{y}$.

Quadrants	Rotation centres
I. $\dot{x} > 0, \dot{y} > 0$	$A_1(k_1 + a, k_2 - b)$
II. $\dot{x} < 0, \dot{y} > 0$	$A_2(k_1 + a, k_2 + b)$
III. $\dot{x} < 0, \dot{y} < 0$	$A_3(k_1 - a, k_2 + b)$
IV. $\dot{x} > 0, \dot{y} < 0$	$A_4(k_1 - a, k_2 - b)$

For brevity sake the centres of rotation A_1, A_2, A_3 and A_4 will further be denoted by the figures *1*, *2*, *3* and *4*, respectively.

The conditions for the transition of the image-point from one quadrant to another and for its motion along the axes $\dot{x}$ and $\dot{y}$ cannot be entered upon here in detail.

At any rate it is not difficult to obtain the path of this point in a plot. It will then be an easy matter by making use of relations (8) to calculate a series of consecutive values assumed by x and y, and, having found from (3) the respective values of α and β, the path of the end-point of the gyroscope axis will readily be obtained.

§ 2. Simple Cases of Gyroscope Motion with Friction on Suspension Axes

In the plane $\dot{x}$, $\dot{y}$ we notice points *10*, *20*, *30* and *40* defined by the coordinates (k_1+a_0, k_2-b_0), (k_1+a_0, k_2+b_0), (k_1-a_0, k_2+b_0), (k_1-a_0, k_2-b_0). The rectangle *1*, *3*, *3*, *4* lies inside the rectangle *10*, *20*, *30*, *40*.

It is easily seen that in case the origin ($\dot{x}=0$, $\dot{y}=0$) lies inside the rectangle *10*, *20*, *30*, *40*, the image-point remains motionless when in the position $\dot{x}=0$, $\dot{y}=0$. Nor does the axis of the gyroscope describe any motion under these conditions. The external moments applied to the gyroscope are counterbalanced by the moments of static friction on the suspension axes.

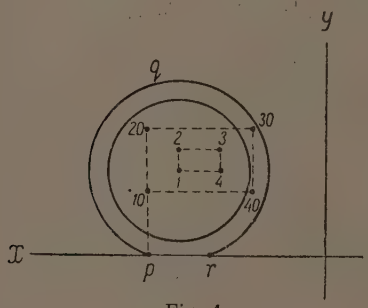

Fig. 1.

Motionless, too, is the image-point when it coincides with one of the rotation centres *1*, *2*, *3* or *4*, provided this rotation centre is itself located within its respective quadrant. In this case the gyros c ope axis is n regular precessional motion.

Suppose the centre of rotation *1* to lie within the first quadrant. Let us draw a circle C which has its centre at point *1* and does not intersect either the axis $\dot{x}$ or the axis $\dot{y}$ (Fig. 1). Suppose further that the initial position of the image-point is on the circumference of this circle. In its subsequent motion the image-point, as we already know, will describe the above-mentioned circumference by uniform rotation about the centre *1* at angular velocity λ. In that case the motion of the gyroscope axis is a pseudo-regular precession in which steady nutational oscillations are superposed to the regular precession $\dot{x}=k_1+a$, $\dot{y}=k_2-b$. The fact that steady nutational oscillations of the gyroscope are possible in face of friction on the axes of the cardan suspension appears at first sight to be a paradox. What

accounts for it, is that here the negative work of the friction moments is offset by the positive work of the external moments applied to the gyroscope.

Let us further draw an arc of circle *pqr* having its centre at point *1* and not intersecting the axis $\dot{y}$ (Fig. 1). It is easy to see that to the closed contour formed by the arc *pqr* and the straight line *rp* also corresponds a periodical motion of the image-point.

Here again we have the gyroscope axis making a pseudo-regular precession with undamped nutational oscillations. This precession is characterized by the fact that the path of the end-point of the gyroscope axis, when depicted on the plane α, β, contains certain rectilinear portions parallel to the axis α.

§ 3. Gyroscope Motion with Arbitrary Initial Data

A constant external moment $M_1 > 0$ about the axis of rotation of the inner ring is supposed to be applied to the gyroscope ($M_2 = 0$, $k_2 = 0$). Denote the initial values of $\dot{x}$ and $\dot{y}$ by $\dot{x}_0$ and $\dot{y}_0$, respectively, and put $\dot{x}_0 > 0$ and $\dot{y}_0 = 0$.

To plot the path of the image-point is a matter of no considerable difficulty (Fig. 2).

It consists of a sequence of circular arcs $C_0 C_1$, $C_1 C_2$, $C_2 C_3$, $C_3 C_4$, $C_4 C_5$,....

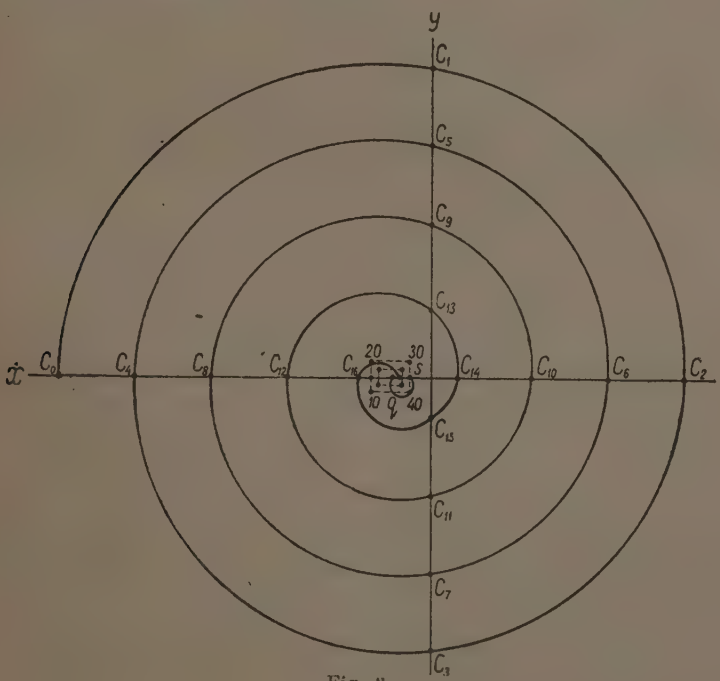

Fig. 2.

having their centres at points *1*, *2*, *3*, *4*, *1*,..... respectively. The sequence ends with the arc $C_{16} C_{17}$ crossing the axis $\dot{x}$ between points *p* and *s* inside the rectangle *10*, *20*, *30*, *40*.

After this the image-point moves uniformly along the $\dot{x}$-axis until point *s* is reached, and then begins its periodical motion along the closed contour made up by the circular arc *sqr* (having its centre at point *4*) and the straight line *rs*.

The last portion of the path of the image-point is represented in Fig. 3 on a magnified scale.

By means of a plot thus constructed (Figs. 2 and 3) a series of consecutive values of x and y is easily calculated from formulae (8), applied to separate sections

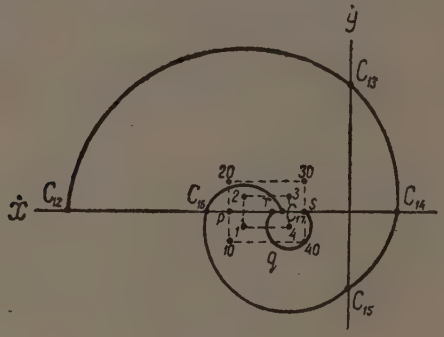

Fig. 3.

$C_0 C_1$, $C_1 C_2$, $C_2 C_3$ etc. of the path of the image-point; and from these values the respective values of angles α and β are derived. In that way the curve f ($\alpha \cos \beta_0$, $\beta = 0$), i. e. the path of the end-point of the gyroscope axis, can be drawn point by point (Fig. 4).

It may be seen that under the influence of friction on the suspension axes the nutational oscillations of the gyroscope axis are damped at first and the damping

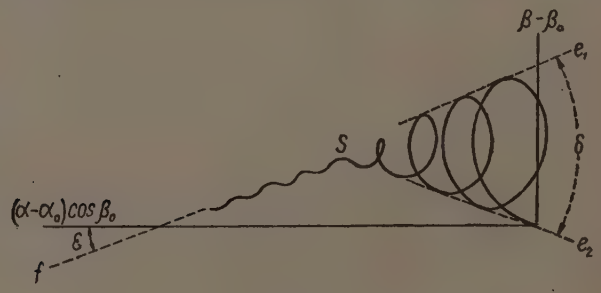

Fig. 4.

continues until point S is reached (Fig. 4). After this steady nutational oscillations of the type mentioned in § 2 are established and the axis of the gyroscope gradually sinks*.

§ 4. Determination of Frictional Moments on the Suspension Axes

If the initial value of $\dot{x}_0$ is high enough compared to k_1, a, b, the lines e_1 and e_2 (Fig. 4) bounding the coils of that portion of the path of the end-point of the gyro-

* The graphs in Figs. 2, 3 and 4 are constructed on the assumption that $\frac{k_1}{b} = 5.5$, $\frac{a}{b} = 1.5$, $\frac{a_0}{b} = 2.5$, $\frac{\dot{x}_0}{b} = 47.4$, $\frac{1}{\cos \beta_0} \sqrt{\frac{B_0}{A_0}} = 1.5$. The gyroscope axis is supposed to be directed to the side, from which the observer sees the proper motion of the gyroscope to proceed clockwise.

scope axis which corresponds to damping, are very nearly straight lines (the coils of the path diminish in all but arithmetical progression). Assuming them to be straight lines, denoting by δ the angle they form with each other and supposing k_1 to be great enough compared to a and b, we obtain as an approximation

$$\operatorname{tg}\frac{\delta}{2}=\frac{2(a+b)}{\pi k_1\cos\beta_0}\sqrt{\frac{B_0}{A_0}}=\frac{2}{\pi M_1\cos\beta_0}\left(K_2+K_1\sqrt{\frac{B_0}{A_0}}\right). \tag{10}$$

On the other hand, for the angle ε formed by the α-axis and the straight line f, about which the end of the gyroscope axis is oscillating while describing that part of its path which corresponds to undamped oscillations, we have

$$\operatorname{tg}\varepsilon=\frac{b}{(k_1-a)\cos\beta_0}\sqrt{\frac{B_0}{A_0}}=\frac{K_2}{(M_1-K_1)\cos\beta_0}. \tag{11}$$

Being given the value of the external moment M_1 and the angle β_0 and having found the angles δ and ε by experiment from the recorded path of the end-point of the gyroscope axis, we can make use of formulae (10) and (11) for determining the moments of friction K_1 and K_2.

Leningrad State University.

Received
14. IX. 1942.

REFERENCES

[1] Е. Л. Николаи, Теоретическая механика, ч. III, гл. IX (1939).

Comptes Rendus (Doklady) de l'Académie des Sciences de l'URSS
1943. Volume XXXVIII, № 2—3

ASTRONOMY

GAS EVOLUTION FROM THE NUCLEUS OF A COMET AS RELATED TO THE VARIATIONS IN ITS ABSOLUTE BRIGHTNESS

By B. J. LEVIN

(Communicated by S. I. Wawilow, Member of the Academy, 22.XII.1942)

1. It has long been firmly established that the formation of gas envelopes and tails at the approach of a comet to the Sun is due to the gases evolved by the nucleus of the comet under the effect of solar heat. The initial state of the gases and the process of their evolution remained, however, rather obscure; some astronomers (see e. g. Kopf in Handbuch der Astrophysik) took care to avoid the subject. One has to admit, it is true, that the problem is no longer obscure with respect to the gases contained in meteorites and even in rocks of the earth crust.

In what follows it is shown that the phenomenon can be explained on the basis of modern data on the sorption of gases by solids (1). If covered with a large number of microfissures any solid body may contain a considerable amount of gases in a sorbed condition. From laboratory data pertaining to diverse gases and adsorbents it is seen that sorption may quantitatively account for the content of gases in rocks of the earth crust.

The kinetic theory of gases makes is possible to calculate the rate of evaporation (volatility) of sorbed molecules, because of the applicability in this case of the formulae of evaporation by solids. The relation between the number of molecules evaporated and the temperature is practically given by the formula (2)

$$n = \text{const}\, e^{-\frac{L}{RT}}, \qquad (1)$$

where L is the heat of sorption per mol; R, absolute gas constant; T, absolute temperature. The constant is proportional to the concentration of the sorbed molecules in the superficial layer. The sorption heats are usually of an order of 5000—10000 cal/mol, i. e. 5—20 times lower that the heat of evaporation of metals and minerals. Hence it is evident that desorption proceeds at much lower temperatures than those necessary for an appreciable evaporation of metals and minerals.

For the case of comets the process may be pictured in the following way; the solid blocks which form the nucleus of a comet contain gases in a sorbed condition. This sorption is of a nature intermediate between adsorption and absorption. In the course of astronomical periods the gases had time to diffuse into separate crystals, and therefore there takes place no rapid desorption when a comet is subjected to the action of solar heat in the neighbourhood of the Sun. On the other hand, however, the gases do not fill the whole volume of crystals being concentrated in the superficial layer*. After the comet had passed the Sun, the surface of these

* Analyses of gas in rocks of the earth crust made by Nikogosian(3) have shown fine-grained rocks to contain 5.6 of gas per volume of solid mineral, while the coarse-grained contain 2 volumes of gas.

crystals which are situated in the heated parts of the nucleus, must be appreciably poorer in sorbed molecules than it was before. By the time of the next approach of the comet to the Sun, the sorbed film may partly be restituted at the expense of inverse diffusion of the molecules from the superficial layer of crystals on the very surface. Moreover, in large blocks, owing to the mobility of this film, there may take place a superficial migration of molecules (along the surface of microcracks) from deeper layers, to which the heat penetrates not until the comet has already receded from the Sun. By this time the blocks are cooled and there is therefore no evaporation of molecules; these stay in place until the next approach to the Sun.

2. The visible radiation of comets is largely due to the resonance bands of C_2. At a given distance from the Sun the light intensity I of the head of the comet is therefore proportional to the total number of C_2 molecules contained in it. The number of C_2 molecules is in its turn proportional to the number n of molecules evaporated per unit time from unit surface; it is also proportional to the mean period the molecules remain within the region of the comet's head (τ). If it is taken into account, moreover, that the density of the solar radiation, which is selectively scattered by the molecules of the comet's head, is inversely proportional to the square of its distances from the Sun, we obtain

$$I \sim \frac{n\tau}{r^2}.$$

Let us assume that the temperature of the parts of the nucleus by which the molecules are evaporated, is expressed by the formula

$$T = \frac{T_0}{\sqrt{r}}$$

(putting T_0 equal to 350°K). Then, according to (1)

$$n \sim e^{-\frac{L}{RT}} = e^{-\frac{L\sqrt{r}}{RT_0}}$$

(the change in the concentration of the molecules during the passage of the comet near the Sun is neglected here).

According to the theory of the head of a comet, $\tau \sim \frac{\bar{v}}{g}$, where $\bar{v}$ is the mean value of the ξ-component of velocity of a projected molecule, and g is the effective repulsing acceleration due to the Sun. In so far as $\bar{v} \sim \sqrt{T}$ and $g \sim \frac{1}{r^2}$, $\tau \sim r^{\frac{7}{4}}$. Consequently,

$$I \sim r^{-\frac{1}{4}} e^{-\frac{L\sqrt{r}}{RT_0}}. \qquad (2)$$

The relation between I and r is expressed by the exponential term, and the power factor plays a subordinate part and can be omitted. The absolute brightness of the head of a comet (stellar magnitude at a distance of one astronomic unit from the earth) is obtained in the shape

$$H = -2.5 \lg I + \text{const} = \frac{1.085L}{RT_0}\sqrt{r} + C = 0.00156\, L\sqrt{r} + C. \qquad (3)$$

This formula has been applied to the numerous observations of the comet of Enke, collected by Holetschek(4).

These observations can be classed into three groups: 1) 53 observations previous to the perihelion for 1786—1868 (weight average 1838); 2) 64 observations previous to the perihelion for 1871—1911 (weight average 1895), and 3) 29 observations following the perihelion for 1822—1911 (weight average 1868). The values of the constants L and C entering (3) have been found for each group by the method of least squares. For sake of comparison the observational data were also treated according to the old interpolation formula

$$H = H_0 + 2.5n \lg r \qquad (4)$$

which lacks physical foundation. To make it more illustrative, C is replaced in the table by H_0, the relative brightness of the comet (stellar magnitude at a distance of one astronomic unit from the Earth and the Sun).

Number of observations	r	Formula (3)			Formula (4)		
		H_0, mg	L	ε, mg	H_0, mg	n	ε, mg
53	0.37—2.08	8.88	6700	0-562	9.07	4.3	0.708
64	0.36—2.05	9.30	6870	0.598	9.51	4.7	0.726
29	0.40—1.25	10.34	7450	0.627	10.35	4.5	0.579

The observations made previous to the perihelion do better fit within the new formula than within the old, the former giving much smaller values of the mean quadratic deviation ε. For observations made after perihelion the new formula yields somewhat larger values of ε. Beyond the perihelion, however, the course of gas evolutions is affected by: 1) the decrease in gas concentration and 2) the temperature inertia of the nucleus. The decrease in gas concentration is evidenced by the fact that the difference in brightness before and after perihelion amounts to 1 mg. The secular decrease in brightness which may be seen from a comparison of group 1 and group 2 is insignificant; this is another evidence that the processes of restitution of the sorbed film take place in the superficial layers of the blocks.

The magnitudes of the heat of sorption obtained from observations of the brightness perfectly agree with the values obtained in the laboratory. The increase in the heat of sorption which corresponds to the transition from group 1 to group 2 is due to the secular decrease in the concentration of the molecules sorbed. The high value of L obtained for group 3 is accounted for by a decrease in concentration which takes place during one passage of the comet nearby the Sun. This is also in full agreement with laboratory data and may be put down to the fact that those molecules, which are the less firmly bound with the surface, are the first to evaporate.

Seven series of observations of Brux' comet (1911 V) due to different astronomers have been treated in the same way. For five series involving the most important variations of r, the new formula yields better interpretation than the old one. The most significant value for L out of those obtained for all the 140 records, is $L = 4690$ cal/mol.

On the whole, the photometrical treatment of observations carried out on comets goes fully to confirm the physical theory put forward in § 1.

In some comets the curve of the dependence of H on r shows a marked kink. This should probably be accounted for by the appearance of some new radiations in the visible spectrum of the comet, which is due to new molecules penetrating the envelopes. A similar effect must be due in particular to the appearance of Na radiation, which takes place in all comets approaching the Sun at a sufficiently short distance.

Received
10.XII.1942.

REFERENCES

[1] Дж. В. Мак-Бэн, Сорбция газов и паров твердыми телами (1934). [2] И. Ленгмюр, Усп. физ. наук, 14, 208 (1934). [3] Х. С. Никогосян, Труды 3 совещ. по эксп. минералогии и петрографии, изд. Ак. Наук (1940). [4] J. Holetschek, Wiener Denkschr., Math.-Nat. Kl., Wien (1896—1905).

Comptes Rendus (Doklady) de l'Académie des Sciences de l'URSS
1943. Volume XXXVIII, № 2—3

ASTRONOMY

INTEGRAL PHOTOMETRY OF THE SOLAR CORONA OF SEPTEMBER 21, 1941 IN DIFFERENT PARTS OF THE SPECTRUM

By N. N. SYTINSKAYA

(Communicated by S. I. Wawilow, Member of the Academy, 10.X.1942)

The aim of the measurements described in this paper was to compare photometrically the illumination (or the so-called «integral brightness») from the corona with the light of the Sun, the Moon and laboratory standards. As an instrument a camera without object glass was made use of. To the camera was attached a black tube supplied with diaphragms, directed towards the corona. With the help of such an arrangement the photographic plate received the light from an area of the sky 5° in diameter, with the solar corona just in the centre of it. The radiation obtained consisted of the light from the corona itself and of the scattered light of the sky.

In order to measure and evaluate the latter, two identical cameras more were directed towards the sky at the altitude of the corona, at a distance of 10° to the left and to the right of it. In the subsequent the brightness of the sky at these points and that of the corona was supposed equal. For the observations «Isochrom» plates were supplied with 4 light-filters in front of each of them, a yellow, a gray, a blue and a violet one.

The observations were carried out at Alma-Ata by V. L. Rabinovich, undergraduate of the Kazakhstan State University; the sky was cloudless. The exposure obtained for all the cameras simultaneously was of 50 seconds. Later on observations were made of the light of a standard lamp with a known candle-power and with a colour temperature $T = 2470°$, as well as of the light of the full Moon and the Sun.

In the latter case the rays were so directed as to fall upon a small screen covered with magnesia. The plate was illuminated by light reflected from an area of this screen limited by a diaphragm, whose radius R was exactly known. If the distance between the diaphragm and the plate be L and the angle of incidence of the solar rays falling upon the screen be i, then the illumination E received by the plate will be:

$$E = E_s r \frac{R^2}{L^2} \cos i,$$

where E_s is the illumination from the Sun on the plane normal to the rays, and r is the reflection factor which in the case of magnesia can be put equal to unity at any part of the spectrum.

A standard scale was obtained photometrically on each plate. This made it possible to obtain illumination from all the bodies observed in arbitrary units

after the plates have been measured with the microphotometer. The illumination from the corona was found by subtracting the sky light from the total light of the corona and the sky.

After this there were obtained ratios between the light of the corona and the photometrical standards mentioned above.

In order to solve the difficulty connected with atmospheric absorption which is subject to variation with the phase of the eclipse, owing to changes in the air condition, the two following assumptions were made: 1) The transparence of the atmosphere during the totality is taken to be the same as before and after the eclipse.

This assumption is supported by photometrical observations of sunlight during partial phases carried out at Alma-Ata. 2) The absorption is supposed not to vary for a given part of the spectrum, provided the observations are carried out on objects at an equal altitude above the horizon, the coefficient of atmospheric transmission measured visually being also the same. The Sun and the Moon were observed exactly at the same altitude as the corona; only those observations were made use of, which had been obtained with a visual coefficient equal to that at the day of the eclipse, viz. $p = 0.836$. The comparison of brightness made under such conditions can be supposed to be unaffected by the influence of atmospheric extinction.

The results are given in the table below.

Filter	Part of spectrum, mμ	Effective wave-length mμ	Corona / Sun	Corona / Full Moon
Yellow	490—630	560	5.3×10^{-7}	0.21
Gray	310—630	—	5.4 »	0.31
Blue	460—590	510	5.2 »	0.38
Violet	310—490	430	5.4 »	0.43

Illumination from the corona for the yellow filter without atmosphere equals 0.056 lux.

The results obtained for the yellow filter do practically coincide with those obtained by W. W. Scharonow from visual observations of the corona. A comparison with observations carried out during the eclipse of June 19, 1936 shows that on September 21, 1941 the corona was but slightly brighter, although its shape was entirely different (the corona of 1941 was of the minimum type).

As a by-product there was obtained a comparison of the light of the Sun and that of the Moon, and of these with the light of a standard lamp.

The results are as follows:

Filter	Sun / Moon	Spherical albedo of the Moon (light-phase curve according to Russel)
Yellow	460000	0.074
Gray	490000	0.069
Blue	620000	0.058
Violet	820000	0.041

For the yellow filter ($\lambda = 560$ mμ) the light constant of the Sun (illumination due to the Sun outside the atmosphere for a parallax 8″.80) equals 143000 lux.

The light constant of the Moon (illumination due to the Moon at phase angle 0°, parallax 57′.0, the parallax of the Sun being 8″.80) equals 0.31 lux.

The ratio of the light of the corona to that of the Sun was found to be the same at all parts of the spectrum; hence the conclusion can be made that the radiation of the corona does not differ from that of the Sun as to spectral distribution. The spectral distribution for the light of the standard lamp being known, we can easily find the ratio of the energy I_{430}/I_{560} for the wave-length 430 and 560 mμ, and therefore the colour index and colour temperature. The following values have been obtained:

Object	I_{430}/I_{560}	Colour index	Colour temperature
Corona	1.000	0.65	6000°
Sun	0.970	0.69	5800
Moon	0.800	0.86	5000
Sky	1.880	—0.05	12500

The above data also go to confirm that the corona and the Sun are of the same colour, whereas the Moon is considerably redder than the Sun; during the totality the colour of the sky is blue, closely approaching that of the day sky (according to data supplied for the latter by E. L. Krinov and W. W. Scharonow, $I_{430}/I_{560} = 1.97$).

Leningrad State University.

Received
30. IX. 1942.

Comptes Rendus (Doklady) de l'Académie des Sciences de l'URSS
1943. Volume XXXVIII, № 2—3

PHYSICS

GENERAL THEORY OF THE FOCUSING ACTION OF ELECTROSTATIC AND MAGNETIC FIELDS

III. THREE-DIMENSIONAL (TWISTED) TRAJECTORIES IN THE PRESENCE OF BOTH AN ELECTROSTATIC AND A MAGNETIC FIELD

By G. A. GRÜNBERG

(Communicated by A. F. Joffe, Member of the Academy, 8.XII. 1942)

1. In the second section of this work(1) I have discussed the possible character of beams formed by electrified particles in an arbitrary three-dimensional electrostatic field. Now the more general case will be considered when a magnetic field as well as an electrostatic field are simultaneously present in space.

Our starting point in solving the problem is again the equation of motion of an electrified particle. Let the magnetic field be characterized by a magnetic potential Ω*. As before, we make use of a local system of coordinates x, y, z with their origin O lying somewhere on one of the trajectories of our beam (principal trajectory), and denote by $\mathbf{e}_1'$, $\mathbf{e}_2'$, $\mathbf{e}_3'$ the unit vectors of the natural trihedron at point O' of a second trajectory. The coordinates of this point are (O, p_2, p_3). Thus, keeping to the previously employed notation, we can write:

$$\frac{d}{dt}\left[m\left(\frac{d\mathbf{r}}{dt}+\frac{d\mathbf{p}}{dt}\right)\right] = -e\,\mathrm{grad}\,\bar{\varphi}' + \frac{e}{c}[\mathbf{v}'\mathbf{H}] =$$
$$= -e\,\mathrm{grad}\,\bar{\varphi}' - e\frac{v'}{c}[\mathbf{e}_1', \mathrm{grad}\,\Omega']. \qquad (1)$$

The last expression is true, because $\mathbf{v}' = v'\mathbf{e}_1'$, where $v' = \sqrt{\Phi(\bar{\varphi}')}$ [see formulae (19) and (20) of the second section] is the absolute value of the velocity of motion along the additional trajectory; $\bar{\varphi}'$ and Ω' are the values of the electrostatic and magnetic potentials, respectively, at the points of this trajectory.

Expansion of $\bar{\varphi}$ and Ω in the neighbourhood of O gives

$$\bar{\varphi} = \bar{\varphi}_0 + x\varphi_1 + y\varphi_2 + z\varphi_3 + \frac{1}{2}x^2\varphi_{11} + xy\varphi_{12} + \ldots + \frac{1}{2}z^2\varphi_{33} + \ldots, \qquad (2)$$

* The justification for this lies in the fact that only the values of the magnetic field H, lying at the points of the beam, are of interest for us. No foreign current is present there, while the field due to the beam itself will be neglected.

and

$$\Omega = \Omega_0 + x\Omega_1 + y\Omega_2 + z\Omega_3 + \tfrac{1}{2}\, x^2\Omega_{11} + xy\Omega_{12} + \ldots + \tfrac{1}{2}\, z^2\Omega_{33} + \ldots, \qquad (3)$$

where the following denotations are introduced:

$$\left.\begin{aligned} &\left(\frac{\partial\bar{\varphi}}{\partial x}\right)_0 = \varphi_1, \left(\frac{\partial\bar{\varphi}}{\partial y}\right)_0 = \varphi_2, \left(\frac{\partial\bar{\varphi}}{\partial z}\right)_0 = \varphi_3, \\ &\left(\frac{\partial^2\bar{\varphi}}{\partial x^2}\right)_0 = \varphi_{11}, \quad \left(\frac{\partial^2\bar{\varphi}}{\partial x\,\partial y}\right)_0 = \varphi_{12} \text{ etc.} \\ &\left(\frac{\partial\Omega}{\partial x}\right)_0 = \Omega_1, \left(\frac{\partial\Omega}{\partial y}\right)_0 = \Omega_2, \left(\frac{\partial\Omega}{\partial z}\right)_0 = \Omega_3, \\ &\left(\frac{\partial^2\Omega}{\partial x^2}\right)_0 = \Omega_{11}, \quad \left(\frac{\partial^2\Omega}{\partial x\,\partial y}\right)_0 = \Omega_{12} \text{ etc.} \end{aligned}\right\} \qquad (4)$$

On some elementary considerations based on differential geometry it is easily found that

$$\left.\begin{aligned} &\mathbf{e}_1' = \mathbf{e}_1 + (p_2' - p_3/\tau)\,\mathbf{e}_2 + (p_3' + p_2/\tau)\,\mathbf{e}_3; \\ &\mathbf{e}_2' = \mathbf{e}_1\,(p_3/\tau - p_2') + \mathbf{e}_2 + \mathbf{e}_3\rho\,(2p_2'/\tau - p_2\tau'/\tau^2 + p_3'' - p_3/\tau^2); \\ &\mathbf{e}_3' = [\mathbf{e}_1'\mathbf{e}_2'] = -\mathbf{e}_1\,(p_3' + p_2/\tau) - \mathbf{e}_2\rho\,(2p_2'/\tau - p_2\tau'/\tau^2 + p_3'' - p_3/\tau^2) + \mathbf{e}_3. \end{aligned}\right\} \qquad (5)$$

If the left-hand side of equation (1) is now expanded in just the same manner, as has been done with equations (14) and (21) in the second section of this work, and on its right-hand side $\{\operatorname{grad}\bar{\varphi}\}_0$, $\{\operatorname{grad}\Omega\}_0$ and $\mathbf{e}_1'$ are substituted with their respective expressions from (2), (3) and (5), we obtain after scalar multiplication by $\mathbf{e}_2$ and $\mathbf{e}_3$:

$$\left.\begin{aligned} &(p_3' + p_2/\tau)\,\frac{d\bar{\varphi}}{ds} + 2\,[p_3'' - p_3/\tau^2 + 2p_2'/\tau - p_2\tau'/\tau^2]\,\bar{\varphi} = p_2\varphi_{23} + p_3\varphi_{33} + \\ &+ \alpha\sqrt{\bar{\varphi}}\left\{-(p_2' - p_3/\tau)\,\Omega_1 + p_2\Omega_{22} + p_3\Omega_{23} + \frac{\Omega_2}{2\bar{\varphi}}\,(p_2\varphi_2 + p_3\varphi_3)\right\}; \\ &(p_2' - p_3/\tau)\,\frac{d\bar{\varphi}}{ds} + 2\,\{p_2'' + p_2\,(1/\rho^2 - 1/\tau^2) - 2p_3'/\tau + p_3\tau'/\tau^2\}\,\bar{\varphi} + \\ &+ p_2\left(\frac{2}{\rho}\,\varphi_2 - \varphi_{22}\right) + p_3\left(\frac{2}{\rho}\,\varphi_3 - \varphi_{33}\right) = \alpha\sqrt{\bar{\varphi}}\left\{(p_3' + p_2/\tau)\,\Omega_1 - \right. \\ &\left. - (p_2\Omega_{23} + p_3\Omega_{33}) - \frac{\Omega_3}{2\bar{\varphi}}\,(p_2\varphi_2 + p_3\varphi_3)\right\}; \\ &\alpha = \frac{1}{c}\sqrt{-\frac{2e}{m}}. \end{aligned}\right\} \qquad (6)$$

Here the relations

$$\bar{\varphi}_{0'} = \bar{\varphi}_0\left(1 + p_2\,\frac{\varphi_2}{\bar{\varphi}} + p_3\,\frac{\varphi_3}{\bar{\varphi}}\right) + \ldots; \qquad (7)$$

$$(\operatorname{grad}\varphi, e_2)_{0'} = \varphi_2 + p_2\varphi_{22} + p_3\varphi_{23}; \quad (\operatorname{grad}\bar{\varphi}, \mathbf{e}_3)_{0'} = \varphi_3 + p_2\varphi_{23} + p_3\varphi_{33}; \qquad (8)$$

$$\left.\begin{aligned} &(\mathbf{e}_2, [\mathbf{e}_1', \operatorname{grad}\Omega])_{0'} = (\operatorname{grad}\Omega, [\mathbf{e}_2, \mathbf{e}_1'])_{0'} = -(\Omega_3 + p_2\Omega_{23} + p_3\Omega_{33}) + \\ &\qquad + (p_3' + p_2/\tau)\,\Omega_1; \\ &(\mathbf{e}_3, [\mathbf{e}_1', \operatorname{grad}\Omega])_{0'} = (\operatorname{grad}\Omega, \mathbf{e}_2 - [p_2' - p_3/\tau]\,\mathbf{e}_1) = \\ &\qquad = (\Omega_2 + p_2\Omega_{22} + p_3\Omega_{23}) - (p_2' - p_3/\tau)\,\Omega_1 \end{aligned}\right\} \qquad (9)$$

have been used and the result is written down for the non-relativistic case*.

Equations (6) are a generalization of equations (26) of the second section of the present work for the case when the electrostatic and the magnetic fields are both present. There exist ten relations between the quantities φ_i, φ_{ij}, Ω_m, Ω_{mn}.

* The corresponding formulae for the relativistic case are evidently not difficult to obtain either.

Four of these relations are obtained from the conditions:

$$\left.\begin{aligned} \frac{\psi(\bar{\varphi})}{\rho} &= (\operatorname{grad}\bar{\varphi}, \mathbf{e}_2) - \frac{1}{c}\sqrt{\Phi(\bar{\varphi})}\,(\operatorname{grad}\Omega, \mathbf{e}_3) \\ (\operatorname{grad}\bar{\varphi}, \mathbf{e}_3) &= -\frac{1}{c}\sqrt{\Phi(\bar{\varphi})}\,(\operatorname{grad}\Omega, \mathbf{e}_2) \end{aligned}\right\} \tag{10}$$

which present a generalization of conditions (1) and (2) of the second section; two are based on the fact that $\bar{\varphi}$ and Ω satisfy each Laplace's equation, and the remaining four follow from $\bar{\varphi}$ and Ω being supposed to be known along the arc s of the principal curve.

So we find, as we did in deriving formulae (5), (7), (8) and (9) of the second section, that

$$\left.\begin{aligned} &\varphi_1 = \left(\frac{d\bar{\varphi}}{\partial s}\right)_0, \quad \varphi_{11} + \frac{1}{\rho_0}\varphi_2 = \left(\frac{d^2\bar{\varphi}}{ds^2}\right)_0; \quad \Omega_1 = \left(\frac{d\Omega}{ds}\right)_0, \\ &\Omega_{11} + \frac{1}{\rho_0}\Omega_2 = \left(\frac{d^2\Omega}{ds^2}\right)_0; \\ &\frac{\psi(\bar{\varphi}_0)}{\rho_0} \equiv \frac{\psi_0}{\rho_0} = \varphi_2 - \frac{1}{c}\sqrt{\Phi_0}\,\Omega_3; \\ &\varphi_3 = -\frac{1}{c}\sqrt{\Phi_0}\,\Omega_2; \quad \Phi_0 \equiv \Phi(\bar{\varphi}_0); \\ &\left[\frac{d}{ds}\frac{\psi}{\rho}\right]_0 = \left(\varphi_{12} - \frac{1}{\rho_0}\varphi_1 + \frac{1}{\tau_0}\varphi_3\right) - \\ &-\frac{1}{c}\left[\sqrt{\Phi_0}\left(\Omega_{31} - \frac{1}{\tau_0}\Omega_2\right) + \frac{\Phi'(\bar{\varphi}_0)}{2\sqrt{\Phi_0}}\left(\frac{d\bar{\varphi}}{ds}\right)_0\Omega_3\right]; \\ &\varphi_{31} - \frac{1}{\tau_0}\varphi_2 = -\frac{1}{c}\left[\left(\Omega_{12} - \frac{1}{\rho_0}\Omega_1 + \frac{1}{\tau_0}\Omega_3\right)\sqrt{\Phi_0} + \right. \\ &\qquad \left. + \frac{\Phi'(\bar{\varphi}_0)}{2\sqrt{\Phi_0}}\left(\frac{d\bar{\varphi}}{ds}\right)_0\Omega_2\right]; \\ &\varphi_{11} + \varphi_{22} + \varphi_{33} = 0; \quad \Omega_{11} + \Omega_{22} + \Omega_{33} = 0. \end{aligned}\right\} \tag{11}$$

Eight of the quantities φ_i, φ_{ij}, Ω_m, Ω_{mn} remain arbitrary functions of s. From this we are led to conclude that in the most general case, namely when electrostatic and magnetic fields are applied together, the number of trajectories, which may be chosen of at pleasure, cannot exceed 6 in contradistinction to the case of the presence of an electrostatic field only, when this number does not exceed two and a half.

2. We shall not enter here into a more curtailed analysis of the general equations (6), but confine ourselves to the examination of the case when a magnetic field alone is present, in which case $\bar{\varphi} = \text{const} \equiv \varphi^0$ everywhere in space.

Suppose, moreover, that the principal trajectory is a plane trajectory, its plane lying midway between two pole shoes N and S similar in form. Under these conditions we obtain from (6)

$$\left.\begin{aligned} p_2'' + \left(\frac{1}{\rho^2} + \frac{\alpha}{2\sqrt{\varphi^0}}\Omega_{23}\right)p_2 = 0, \\ p_3'' - \frac{\alpha}{2\sqrt{\varphi^0}}\Omega_{23}p_3 = 0, \end{aligned}\right\} \tag{12}$$

for then, by virtue of symmetry,

$$\Omega_1 = \Omega_2 = 0; \quad \Omega_{11} = \Omega_{22} = \Omega_{12} = 0, \tag{13}$$

and from the equation of Laplace it follows that $\Omega_{33} = 0$ also. The equations for p_2 and p_3 are thus separated, and focusing is ensured in all cases (cf. paragraph 6 of the second section). One should also note that for the

principal curve there always take place the relations (10), of which the first in the case considered turns simply into

$$\frac{\sqrt{2\varphi^0}}{\rho} = -\alpha\Omega_3 = \alpha H_z, \tag{14}$$

and the second is satisfied automatically.

If the field **H** is so chosen that $\frac{\alpha}{2\sqrt{\varphi^0}}\Omega_{23} = -\frac{1}{2\rho^2}$, equations (12) transform into

$$p_2'' + \frac{1}{2\rho^2}p_2 = 0, \qquad p_3'' + \frac{1}{2\rho^2}p_3 = 0, \tag{15}$$

which means that in this case $p_3 = p_2$.

3. To sum up, the method suggested in the present work affords the possibility for dealing in the most general way with problems in which the focusing of electron and ion beams of any desired type is considered. By using it it is also possible to decide to what extent such focusing beams are arbitrary and to establish the character of electrostatic and magnetic fields necessary for their creation. The questions concerned with focusing of the first order (narrow beams) are explored in the most general way, and there are also examined some special cases, in which the shape of the fields required for actually effecting the focusing can be determined with particular ease.

Leningrad Physical-Technical Institute.
Academy of Sciences of the USSR.

Received
7. XII. 1942.

REFERENCES

[1] G. A. Grünberg, C. R. Acad. Sci. URSS, XXXVII, No. 9 (1942).

Comptes Rendus (Doklady) de l'Académie des Sciences de l'URSS
1943. Volume XXXVIII, № 2—3

TECHNICAL PHYSICS

PIEZOELECTRIC SURGICAL PROBE

By V. A. OSTROUMOV and V. N. LEPESHINSKAYA

(Communicated by S. I. Wawilow, Member of the Academy, 19.IX.1942)

It is well known that during a surgical operation the surgeon depends chiefly upon his sense of touch. His sight cannot penetrate into a deep wound, while X-ray photographs are usually taken before the operations. His work would be greatly facilitated, however, by the assistance of such a perfect and developed organ as our organ of hearing. The way to this is opened by the extremely high piezoelectric sensitiveness of the rochell salt which is not inferior to our sense of touch.

A plate cut out in the proper way from a crystal of rochell salt and covered on both sides by metallic sheets will give on the sheets, even in the case of the smallest elastic strains, opposite electric charges which, being transmitted by wires to the sheets of a second plate, cause mechanical strains in the latter, these strains being similar to the strains of the first plate, caused by outer forces.

In this phenomenon we have the reversibility of the piezoelectric effect which enables to apply it both to the transformation of mechanical oscillations into electrical and, reversely, to excite mechanical oscillations, including sound, with the aid of electric ones. In other words, it allows the construction of piezoelectric microphones and telephones differing but little from each other in construction.

Of course, the charges arising in a piezoelectric microphone can be amplified with the aid of a vacuum tube, and owing to the high sensitiveness and great efficiency of a piezoelectric telephone we can confine ourselves to the amplification of the potential, whereby the construction of the amplifying device is considerably simplified, and reduced to only one or two stages of amplification.

The peculiarity of the piezoelectric effect in the rochell salt compels us to use, instead of simple single plates, complicated ones made of two plates glued together. In these plates two electrodes, connected with each other, are fastened by glueing to the outer faces and a third electrode connected with the outer circuit is placed between the plates. Such a complicated plate, called a «bimorphous element», is the most suitable one for a reciprocal transformation of mechanical and electrical oscillations and has a greatest sensitiveness. The slightest touch is already sufficient for the appearance of charges in the microphone, and insignificant electric oscillations (with an amplitude of several millivolts) in the piezotelephone give a sound loud enough to be heard by ear.

These considerations led to the construction of a new instrument, the piezoelectric surgical probe, which permits an examination of sounds more careful and many-sided than with an ordinary probe, so that the presence of foreign bodies (fragments of shells, pieces of bones, small stones, etc.) can be detected in a deep wound.

When the point of the probe will touch some solid object, even small in size, in the wound, an electric sound wave will arise in the metal body of the probe;

the damping of this wave takes place not too quickly, since, on the one hand, its amplitude is not great and, on the other, the dissipation of the oscillation energy from the steel rod of the probe to the tissues surrounding it and into the hand of the surgeon is hampered as a result of the great difference between the acoustic properties of steel and soft tissues of the human body and because of a relatively small pressing of the metal to these soft tissues.

In such a way the rod of the probe turns out to be an excellent conductor of acoustic waves, these waves being of small amplitude and high frequency.

If we connect rigidly to the handle of the probe a bimorphous piezoelectric element of rochell salt, similar to the ones used in piezoelectric measuring microphone, even the most insignificant sound oscillations and vibrations will cause in it corresponding electric oscillations; these oscillations being slightly amplified, and in some cases even without amplifying, will be fully sufficient for the excitation of a sensitive piezoelectric telephone of a membrane type.

It is evident that the peculiarities of the surface of the foreign body, whether it is smooth or rough, of metal or of some other material, absolutely free or covered by some film, will all be represented by the variety of characters of sound heard in the telephone.

Our sense of hearing in such a way will serve to widen the tactile impressions and to make them more exact, and will enable the surgeon to probe the wound much more quickly and with less exertion and to proceed to the operation with more certainty.

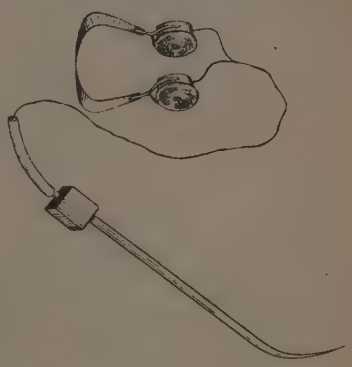

Fig. 1.

At present we have two models of such surgical probes (developed in the Leningrad Medico-Pediatric Institute, in the Department of Physics). The first model—without any amplifying—is based, chiefly, on the sharpness of our sense of hearing and on the high sensitiveness of piezoelectric instruments.

It consists of a small rigid box in which the bimorphous element is placed and which is rigidly attached by means of screws to the handles of ordinary surgical probes (Fig. 1).

A conducting wire from the bimorphous element transmits the electric oscillations to the head piezoelectric telephone which not only enables the surgeon to hear the vibrations of the probe, but also covers his ears and thus protects him from all external noises, helping him in this way to concentrate his attention on the work of the probe.

The weight of this device is insignificant; it fits well into a pocket or into a case of a field-set of surgical instruments.

This model is intended mainly for work under field conditions in a fighting army; it needs no batteries or other sources of feeding, being a, relatively, crude elementary instrument.

The second model differs from the first in having a single tube amplifier, with the lightest possible feeding batteries of minimal commercial size, introduced between the probe and the head telephone (Fig. 2).

In constructing this kind of amplifier the penthode 2K2M or CO-241 can be used expediently, for they allow to use, for feeding purposes, the lightest available dry batteries (BAS-60 and BAS-40) and to bring down the size of the amplifier to that of a cigarette case (a scheme of such an amplifier is given in Fig. 2). Here we can increase the amplification several 100 times with respest to potential difference, and correspondingly raise the sensitiveness of the instrument.

It is not difficult to increase the amplification still further by introducing a second tube, but usually there is no need for that.

By only glancing at the scheme of the amplifier it is not difficult to see that

it allows a wide range of frequencies. On the other hand, piezoelectric instruments, in particular telephones, are suitable for reproduction of high frequencies. These two circumstances make the instrument especially adapted for discovering rustles and noises and, on the other hand, decrease its sensitivity to musical tones of lower frequencies. Thus, the instrument is sensitive only to insignificant vibrations of the probe when it meets a foreign body, and remains insusceptible to the sounds

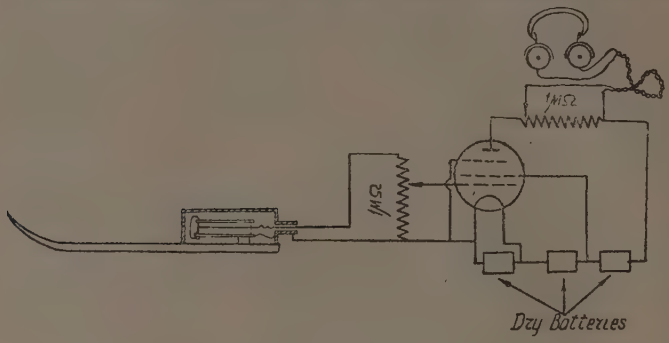

Fig. 2.

in the room; one is struck by this quality from the first attempts to work with the instrument.

Evidently, it is very useful to heighten the sense of touch of the surgeon not only during the probing of the wound, but also during the operation itself, especially if he has to work in the vicinity of bones or to extract fragments of shells.

The piezoelectric element may be rigidly attached to the handle of any surgical instrument, for instance of a lancet. It is evident that the lancet will vibrate differently when cutting the different tissues or fascias, or, especially, when meeting solid objects, and our ear will be able to follow the penetration of the lancet into the tissues of the organism.

In this case, too, hearing comes to the aid of motor and tactile perceptions.

Department of Physics.
Leningrad State Pediatric and
Medical Institute.

Received
19. IX. 1942.

Comptes Rendus (Doklady) de l'Académie des Sciences de l'URSS
1943. Volume XXXVIII, № 2—3

CHEMISTRY

X-RAY ANALYSIS OF A NEW TYPE OF COMPLEX COMPOUNDS OF TETRAVALENT PLATINUM

By A. M. RUBINSTEIN and V. G. KUZNETZOV

(Communicated by V. G. Chlopin, Member of the Academy, 19.IX.1942)

In 1940 A. M. Rubinstein (1) obtained by the catalytic decomposition of the pentammine of Chugaev $(NH_3)_5\,ClPtCl_3$, a new type of complex compounds of tetravalent platinum in which two molecules, the salt of Gros $(NH_3)_4\,Cl_2PtCl_2$ and the amide of the tetrammine $(NH_3)_4NH_2ClPtCl_2$, both saturated with respect to coordination bonds, form a new compound having the composition: $(NH_3)_4NH_2ClPtCl_2.(NH_3)_4Cl_2PtCl_2$.

The chemical and the optical properties of this compound (1), its electroconductivity (2) and thermal stability (3) showed this substance to be a typical chemical compound of strictly constant composition and with quite definite properties.

These investigations showed as well quite clearly the difference existing between the properties of the new compound and those of the components it had been formed from, as well as of their mechanical mixture. Optical and chemical properties pointed as well at the impossibility of considering the substance obtained as a solid solution, in which one of the two components is the solvent with respect to the other. It seemed worthy of interest to check these conclusions by means of a comparative study of powdergrams. With this purpose in mind we obtained X-ray photographs for the powders of pure components—the salt of Gros and the amido-tetrammine, of which the new compound was composed; for their mechanical mixture, containing 51.22% of the salt of Gros and 48.78% of the amido-tetrammine; for the pentammine of Chugaev as the initial salt, and for the new salt $[(NH_3)_4NH_2ClPtCl_2][(NH_3)_4Cl_2PtCl_2]$.

The photographs were obtained with iron radiation in chambers according to Debye; the diameter of the plate-holder was 56.2 mm, the film was mounted in it according to Straumanis. The irradiated samples were cylinders, 0.3—0.4 mm in the diameter. They were obtained by fastening the powdered substance upon a thin glass capillary by means of collodion. During the exposure the samples were rotated.

The exposure lasted 5—6 hours, at 8 mA and 30 kV. The individual compounds and their mechanical mixture gave fairly legible X-ray spectrograms, but the lines of the new salt were of poor intensity.

Even on visual comparison there could be noticed quite distinct differences between the salt of Gros, the amide of the tetrammine, the pentammine of Chugaev and the new salt, as reflected in the spectrograms. As for the mechanical mixture, its spectrogram was identical with that of the salt of Gros, but for a series of additional lines due to the amide of the tetrammine.

The new compound gave a different spectrogram from that of the mechanical mixture of components.

This was borne out by computations based on the X-ray photographs obtained and by the results of deciphering the lines of the mechanical mixture.

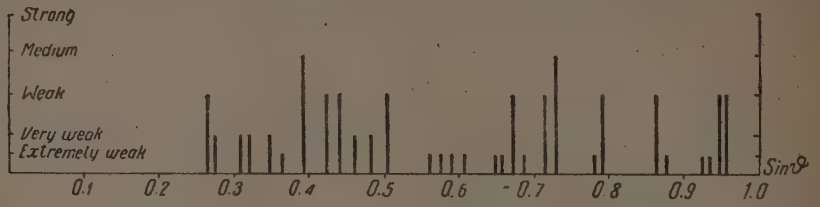

Fig. 1. Salt of A. M. Rubinstein $(NH_3)_4Cl_2\,PtCl_2$. $(NH_3)_4\,NH_2ClPtCl_2$.

What has been obtained in this way is shown in the table. Here for the sake of comparison sines of the Bragg's glancing angles, attended by indications as to the intensity of lines, are listed for all the investigated substances.

It follows clearly from this table that many lines of the salt of Gros and of amide of the tetrammine coincide. On the X-ray photographs of the mechanical mixture these lines merge into common lines. But there are also lines characteri-

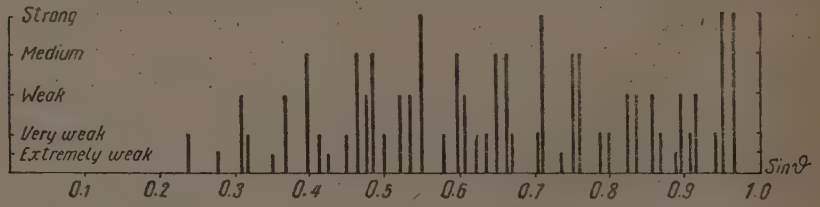

Fig. 2. Mixture of salt of Gros and the amide of the tetrammine (50%+50%).

stic of one of the components that are not characteristic of the other component.

This shows that the salt of Gros and the amide of the tetrammine have very close crystalline structures.

No direct determination of crystalline structure has been made, because there are serious difficulties in the way of obtaining monocrystals of necessary dimensions.

Certain lines of the new salt came near in intensity and in the magnitude of sin ϑ to the lines of the mechanical mixture. But this coincidence is rather a matter of chance.

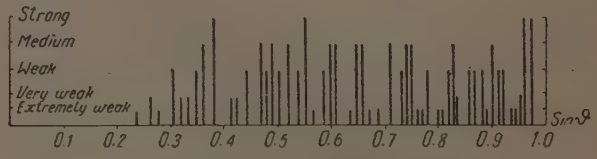

Fig. 3. Salt of Gros $(NH_3)_4Cl_2\,PtCl_2$.

As it may be seen from the table, the majority of lines does not coincide either in the magnitude of sin ϑ or in intensity. Many lines of the mechanical mixture between the salt of Gros and the amide, among them lines of strong and medium intensity, have not even near values to those of the line of the new salt. Such are the medium intensity line of the mechanical mixture

X-ray diffraction lines of the salt of Gros and the amido-tetrammine			X-ray diffraction lines of mechanical mixture 51.22% of the salt of Gros and 48.78% of the amide			X-ray diffraction lines of the new double salt		X-ray diffraction lines of Chugaev's pentammine	
Intensity	sin ϑ	Phases	Intensity	sin ϑ	Phases	Intensity	sin ϑ	Intensity	sin ϑ
1	2	3	4	5	6	7	8	9	10
extremely weak	0.2433	amide	—	—	—	—	—	—	—
do	0.2466	Gros	—	—	—	—	—	—	—
								very weak	0.2520
weak	0.2640	amide	very weak	0.2641	amide Gros	weak	0.2604		
very weak	0.2656	Gros							
						very weak	0.2706		
extremely weak	0.2776	do							
			do	0.2795	do			weak	0.2812
very weak	0.2777	amide							
do	0.2896	do							
medium	0.3049	do							
			weak	0.3068	do	do	0.3078		
weak	0.3065	Gros						do	0.3050
very weak	0.3183	do				do	0.3179		
			do	0.3186	do				
medium	0.3202	amide						extremely weak	0.3287
very weak	0.3352	Gros							
do	0.3353	amide							
								medium	0.3387
do	0.3504	do				do	0.3512		
weak	0.3535	Gros							
medium	0.3702	do							
			weak +	0.3704	do	extremely weak	0.3661		

X-ray diffraction lines of the salt of Gros and the amido-tetrammine			X-ray diffraction lines of mechanical mixture 51.22% of the salt of Gros and 48.78% of the amide			X-ray diffraction lines of the new double salt		X-ray diffraction lines of Chugaev's pentammine	
Intensity	sin ϑ	Phases	Intensity	sin ϑ	Phases	Intensity	sin ϑ	Intensity	sin ϑ
1	2	3	4	5	6	7	8	9	10
medium	0.3703	amide							
strong	0.3867	do						weak	0.3737
do			medium	0.3886	Gros			medium	0.3885
do	0.3883	Gros							
						medium	0.3939		
weak	0.4145	amide							
very weak	0.4178	do	very weak	0.4147	amide				
			extremely weak	0.4260	Gros				
do	0.4257	Gros							
						weak	0.4261		
weak	0.4388	amide						very weak	0.4291
do	0.4417	Gros							
extremely weak	0.4435		very weak	0.4452	do				
						do	0.4452		
strong	0.4657	amide						extremely weak	0.4467
			medium	0.4674	amide Gros				
medium	0.4671	Gros							
						very weak	0.4683	medium	0.4686
weak	0.4797	do							
			weak	0.4808	do				
medium	0.4798	amide							
do	0.4845	do							
			medium	0.4878	do	do	0.4874		
do	0.4890	Gros							
weak	0.5014							do	0.4955
			very weak	0.5002	do				
do	0.5016	amide							
						weak	0.5043		
								weak	0.5169
medium	0.5213	Gros							

X-ray diffraction lines of the salt of Gros and the amido-tetrammine			X-ray diffraction lines of mechanical mixture 51.22% of the salt of Gros and 48.78% of the amide			X-ray diffraction lines of the new double salt		X-ray diffraction lines of Chugacv's pentammine	
Intensity	sin ϑ	Phases	Intensity	sin ϑ	Phases	Intensity	sin ϑ	Intensity	sin ϑ
1	2	3	4	5	6	7	8	9	10
			weak	0.5231	amide				
very weak	0.5245	amide			Gros				
weak	0.5379	Gros	do	0.5367	do			medium	0.5351
medium	0.5500	amide						weak	0.5501
			strong	0.5531	amide				
strong	0.5428	Gros			Gros				
extremely weak	0.5660	do	—	—					
very weak	0.5823	amide				extremely weak	0.5670	weak	0.5693
						do	0.5800		
			weak	0.5854	do				
weak	0.5836	Gros							
do	0.5953	amide						medium	0.5881
			medium	0.5969					
medium	0.5965	Gros				extremely weak	0.5957		
do	0.6095	amide				do	0.6084		
			weak	0.6096	do				
do	0.6107	Gros						weak	0.6124
very weak	0.6304	amide	very weak	0.6237	amide				
extremely weak	0.6385	Gros	do	0.6389	Gros				
						extremely weak	0.6469		
medium	0.6494	do							
			medium	0.6498	do	do	0.6537		
do	0.6628	do							
			do	0.6631	do				
					amide				
do	0.6644	amide							
			very weak					strong	0.6610
extremely weak	0.6734	Gros		0.6692	Gros	weak	0.6722		
								weak	0.6724
do	0.6903	do	—	—	—	extremely weak	0.6878		

X-ray diffraction lines of the salt of Gros and the amido-tetrammine			X-ray diffraction lines of mechanical mixture 51.22% of the salt of Gros and 48.78% of the amide			X-ray diffraction lines of the new double salt		X-ray diffraction lines of Chugaev's pentammine	
Intensity	sin ϑ	Phases	Intensity	sin ϑ	Phases	Intensity	sin ϑ	Intensity	sin ϑ
1	2	3	4	5	6	7	8	9	10
			very					weak	0.6945
weak +	0.7059	amide	weak	0.7058	amide				
medium	0.7095	Gros	strong	0.7087	Gros				
						weak	0.7167	very weak	0.7135
weak	0.7355	do	extremely weak	0.7357	do	medium	0.7287	do	0.7258
medium	0.7426	amide							
			medium	0.7465	amide			medium	0.7452
do	0.7460	Gros			Gros				
very weak	0.7522	amide	—	—					
								very	
medium	0.7566	Gros	medium	0.7582	do			weak	0.7650
extremely weak	0.7658	do	—	—					
do	0.7794	do	—	—					
do	0.7795	amide							
								do	0.7808
						very weak	0.7810		
weak	0.7882	Gros	very weak	0.7887	Gros				
						weak	0.7898		
extremely weak	0.7991	do							
			do	0.8006	amide Gros				
do	0.8036	amide						medium	0.8057
do	0.8128	Gros	—	—					
weak	0.8230	do	weak	0.8234	do				
very weak	0.8238	amide	—	—	—				
								extremely weak	0.8273
medium	0.8340	Gros	weak	0.8343	Gros				

X-ray diffraction lines of the salt of Gros and the amido-tetrammine			X-ray diffraction lines of mechanical mixture 51.22% of the salt of Gros and 48.78% of the amide			X-ray diffraction lines of the new double salt		X-ray diffraction lines of Chugaev's pentammine	
Intensity	sin θ	Phases	Intensity	sin θ	Phases	Intensity	sin θ	Intensity	sin θ
1	2	3	4	5	6	7	8	9	10
very weak	0.8379	Gros	—	—	—				
								medium	0.8440
weak	0.8586	do	weak	0.8572	Gros			do	0.8534
						weak	0.8639		
do	0.8703	do							
			do	0.8698	do				
					amide				
extremely weak	0.8705	amide						medium	0.8749
						extremely weak	0.8761		
weak	0.8797	Gros	weak	0.8801	Gros				
extremely weak	0.8872	do	extremely weak	0.8876	do			weak	0.8875
medium	0.8953	do	weak	0.8957	do				
extremely weak	0.9048	amide	—	—					
weak	0.9099	Gros	extremely weak	0.9095	do				
extremely weak	0.9173	amide							
			weak	0.9174	amide				
					Gros				
								medium	0.9152
weak	0.9178	Gros							
extremely weak	0.9314	do		—		extremely weak	0.9276		
								do	0.9296
do	0.9358	do	—	—		do	0.9360		
			very						
very weak	0.9443	do	weak	0.9443	do				
								extremely weak	0.9480
medium	0.9519	amide							
						weak	0.9506		
			strong	0.9536	amide				
					Gros				
strong	0.9537	Gros							
extremely weak	0.9602	amide	—	—		do	0.9595		
								medium	0.9612
strong	0.9681	Gros	strong	0.9683	o				

sin $\vartheta = 0.3886$, the strong one sin $\vartheta = 0.5531$, the lines of medium intensity sin $\vartheta = 0.6631$, 0.7465, 0.7582, the strong line sin $\vartheta = 0.9683$, etc. Some lines of the new salt are absent in the mechanical mixture.

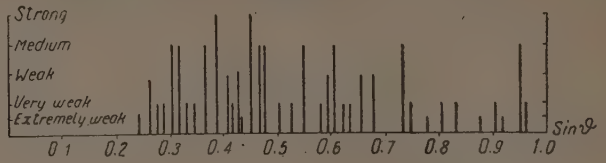

Fig. 4. Amide of the tetrammine $(NH_3)_4NH_2ClPtCl_2$.

Similar picture is observed on the X-ray photographs of the new salt and of the pentammine of Chugaev. By plotting the lines obtained in the X-ray photographs, as is done in Figs. 1—5, the differences existing between the different substances are brought more forcibly out than they appear on the photographs themselves.

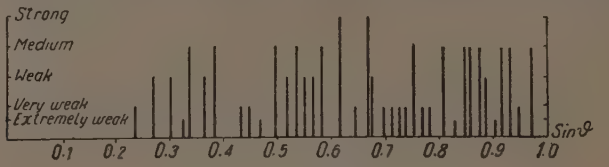

Fig. 5. Pentammine of Chugaev $(NH_3)_5ClPtCl_3$.

X-ray analyses confirm the fact that the new salt, having the composition $(NH_3)_4Cl_2PtCl_2 \cdot (NH_3)_4NH_2ClPtCl_2$, is an individual chemical compound with a typical crystalline structure.

Institute of General and Inorganic Chemistry.
Academy of Sciences of the USSR.

Received
19. IX. 1942.

REFERENCES

[1] A. M. Rubinstein, C. R. Acad. Sci. URSS, XXVIII, No. 1 (1940). [2] А. М. Рубинштейн, Диссертация (1940). [3] А. В. Николаев, А. М. Рубинштейн, Изв. Отд. Химич. наук, № 5 (1940).

Comptes Rendus (Doklady) de l'Académie des Sciences de l'URSS
1943. Volume XXXVIII, № 2—3

GEOCHEMISTRY

A RAPID METHOD FOR DETERMINING Al_2O_3 IN A NEPHELINE CONCENTRATE

By B. N. MELENTIEV

(Communicated by A. E. Fersman, Member of the Academy, 23.X.1942)

While studying the method of phase analysis in relation to apatite-nepheline rocks (1), I found it to be of value as a means of controlling the production of the Apatite-Nepheline Dressing Plant.

In this establishment the quality of a nepheline concentrate is used to be appraised by its content of alumina. The control is carried out in the following way. A weighed sample of the nepheline concentrate is fused with Na_2CO_3, passed into solution by treating the melt with hydrochloric acid; titanium and iron are precipitated by caustic alkali. The precipitated hydroxides are then dissolved and the precipitation repeated. The filtrates are united and acidified. Aluminium is separated in the form of hydroxiquinolate. Last comes the estimation which is made by volume. The nepheline concentrate has a firly stable mineralogical composition. This fact is confirmed by the data on its content of Al_2O_3 which have been accumulating for a rather long period, ever since the plant was set at work. The quantitative mineralogical composition of the nepheline concentrate is referred to in Table 1.

Table 1

No. of samples	Content in %			
	Nepheline	Feldspars	Apatite	Aegirine, sphene, mica and other minerals
4781	86.2	9.4	0.7	4.5
4781	87.0	8.9		4.2
5748	84.5	8.3		7.6
5748	85.2	8.3		7.5
1559	85.2	7.5		5.3
1559	84.7	8.8		7.5
1546	86.0	8.1		8.6

It is seen that the minerals composing the nepheline concentrate fall into two broad groups. In the first belong minerals with a density less than 2.8. These are nepheline and the feldspars. The second group includes nearly all of the remaining minerals entering into the composition of the concentrate. Their density is above 2.8.

Since it is the gross content of Al_2O_3 that is determined by chemical analysis, and this is mainly contained in nepheline and feldspars, it will be obvious that

as soon as the content of this group of minerals is known, the content of alumina can easily be established.

On this consideration and also taking into account the fact that the rock is almost completely disintegrated by crushing*, I thought it fit to apply the method of centrifuging to the new nepheline concentrate in bromoform. This process leads to the formation of two fractions of minerals. The first is the «light» fraction, its density is under 2.8. The second, «heavy» fraction has a density upward of 2.8. After weighing the light fraction it is possible by means of an empirical coefficient to pass from mineralogical data to the content of Al_2O_3 in the concentrate. For that purpose I used an electric centrifuge of ordinary laboratory type, made in the Golitzyno factory, with a motor of 120 volt and a power of 360 watt.

The empirical factor was derived from the content of light fraction, as determined in 17 different samples of the concentrate. In Table 2 are given the results of 10 estimations out of the 23 made.

Table 2

Al_2O_3 in Nepheline Concentrate

No. of samples	Al_2O_3 in %, according to data of Apatite-Nepheline Dressing Plant	«Light» fraction in %	«Light» fraction (Al_2O_3)	Al_2O_3 in %, as derived by means of conversion factor 3.151	Δ
4781	30.27	95.6	3.158	30 34	+ 0.07
4781	30.27	95.9	3.168	30.43	+ 0.16
4781	30.27	94.9	3.135	30.12	— 0.15
5748	29.72	93.8	3.156	29.77	+ 0.05
5748	29.72	92.8	3.123	29.45	— 0.27
5748	29.72	93.5	3.146	29.67	— 0.05
1559	29.56	92.7	3.136	29.42	— 0.14
1559	29.56	93.5	3.163	29.67	+ 0.11
581	29.58	93.8	3.171	29.77	+ 0.19
581	29.58	93.5	3.161	29.67	+ 0.09

In column two is given the content of Al_2O_3, as established directly by the chemical method. The data of the third column bring out the content of the light fraction found by centrifuging. In the fourth column are listed the ratios of the light fraction to the corresponding content of Al_2O_3. And the figures for the content of Al_2O_3 placed in column five have been derived by means of the conversion factor 3.151, which is the average of the data listed in column four.

Table 3

Mean Deviations and Their Distribution

Range of deviation	Deviation from chemical analysis data (σ_1)			Deviation from mean content of Al_2O_3 in nepheline concentrate according to phase analysis (σ_2)			Deviation from mean content of Al_2O_3 in nepheline concentrate accord. to chem. analysis (σ_3)		
	deviation limit in abs. %	number	% to total number of observations	deviation limit in abs.%	number	% to total number of observations	deviation limit in abs. %	number	% to total number of observations
$>\pm 3\ \sigma$	0.84	2	9.1	1.05	0	0	1.50	0	0
$\leqslant\pm 3\ \sigma$	0.84	1	4.5	1.05	2	9.0	1.50	0	0
$\leqslant\pm 2\ \sigma$	0.56	7	31.8	0.70	3	13.6	1.00	16	38.1
$\leqslant\pm\ \sigma$	0.28	12	54.6	0.35	17	77.4	0.50	26	61.9

* This has been confirmed by P. N. Chirvinsky who examined it under the microscope.

When these results were subjected to statistical analysis, the data on Al_2O_3 obtained by means of centrifuging showed an absolute mean quadratic deviation (σ_1) of $\pm 0.28\%$ from the data obtained by the chemical method. It was also found that 86.4% of the data kept within the limits of $\pm 2\sigma_1 = 0.56\%$ (Table 3).

The absolute mean quadratic deviation from the average content of Al_2O_3 in the tested samples of the nepheline concentrate is $\sigma_2 = \pm 0.35\%$ in the case of phase analysis; $\sigma_3 = \pm 0.50\%$ in the case of chemical analysis.

It will be obvious that the indirect method of determining Al_2O_3 in nepheline concentrate is not inferior in respect to accuracy to the chemical method.

As for the time required to carry this process out, it is made up by the length of the following items.

1. Sampling and weighing the filter	10 min.
2. Adjusting the apparatus	10 »
3. Centrifuging	25 »
4. Filtration	20 »
5. Drying	20 »
6. Keeping the sample in the weighing room	15 »
7. Weighing	5 »
Total...	1 hour 45 min.

The method was tried by P. A. Tiutnev on the usual material in the laboratory of the Apatite-Nepheline Dressing Plant. And though the conditions of centrifuging were different, the results were again favourable. He obtained a different empirical modul (3.208) by which he determined the content of Al_2O_3 in the nepheline concentrate. Besides the concentrate, he used other products of the plant as the source of his data.

Received
23. X. 1942.

REFERENCES

[1] А. И. Володченкова и Б. Н. Мелентьев, Изв. Акад. Наук, серия геологич., вып. 1, 141 (1941).

Comptes Rendus (Doklady) de l'Académie des Sciences de l'URSS
1943. Volume XXXVIII, № 2—3

PLANT PHYSIOLOGY

EXPERIMENTAL ELIMINATION OF DORMANCY IN TAU-SAGHYZ

By A. A. SMOLIN

(Communicated by A. A. Richter, Member of the Academy, 4.X.1942)

Plants' period of rest must be regarded as their adaptive reaction to unfavourable conditions of environment (1).

Discrimination is made between winter and summer periods of dormancy. The first is mainly connected with low temperatures, such as prevail in winter, whereas the second is due to drought, which temporarily checks the growth of plants.

Even if the period of dormancy is an adaptive reaction to a whole set of conditions, nevertheless one of the elements of that complex may turn out to be decisive and bring about dormancy at a time when other factors are favourable for vegetation (2).

Some rubber plants, for instance, are liable to pass into dormancy in summer. Tau-saghyz is among their number. All of its forms within their habitat are at rest during the period of summer drought when the temperature continues high. Similar behaviour is shown by this plant at high temperatures in the irrigated regions and oases of Central Asia. In the forest zone the temperature is lower and no form of tau-saghyz is observed there to be at rest in summer, if the amount of moisture is sufficient(2).

From the economical point of view the summer period of dormancy is, of course, an undesired phenomenon, since it prevents the plant from growing for a longer period and thus interferes with the accumulation of vegetative mass.

Very little, if anything at all, is known of the physiological and biochemical modifications taking place in a tau-saghyz plant while in the state of dormancy. On the theory of cyclic ageing and rejuvenation (3), the whole developmental process in plants is a process of ageing or a gradual decrease of the potential of their life-activity, which ends in death.

It is not a rectilinear process, however, but rather a cyclic one, continually interrupted by rejuvenation, whereby the potential of life-activity is temporarily increased.

A variety of unfavourable environmental conditions, such as high temperature attended by deficiency of moisture, make for acceleration of ageing. And it is by removing them that we can further the growth of plants and raise their potential of life-activity.

According to the theory of phasic development (4), the growing points of the stem in a plant are its phasically older parts. Since the leaves are the organs, in which the processes of metabolism are the most intensive, it is easy to understand that they should contain the older tissues, which must have a specific influence on the general development of the plant.

So by cutting the leaves we remove the older tissues. And to remove the phasically older leaves in tau-saghyz at a certain period of its development, for instance,

when it is about to fall into dormancy, means therefore to prevent the imminent inhibition of its further growth. In horticultural practice this kind of rejuvenation has been in use for a long time.

A wounded plant secretes, at the site of formation of the wound, certain growth substances [wound hormones, according to Haberlandt (5)] which stimulate the metabolism towards the mobilization of energy laden plastic substances, out of which a new mass of protoplasm is formed. This restores the growth processes of the plant and permits it to escape the period of dormancy.

Along with nutrient substances water is extremely essential for intensive growth. Therefore water must be supplied to tau-saghyz plants during this period.

These are briefly the theoretical premises upon which have been based the agricultural measures described below. They were designed to break dormancy in the tau-saghyz plants growing at the First Rubber Plant State Farm, the Turkestan district of the Kazakh Autonomous Soviet Socialist Republic.

The fact that the removal of leaves in tau-saghyz plants is apt to break their dormancy was recorded by me as early as in 1938.

In 1940 I started special experiments under industrial conditions on a 1.57 hectare plantation of two-year-old tau-saghyz plants sown in the spring of 1939. They were run according to the following scheme:

Experimental lot	Area in ha
Leaves removed, irrigation	0.50
No removal of leaves, irrigation	0.56
No removal of leaves, no irrigation (control)	0.51

The control was under usual conditions of cultivation, since it is a common practice with tau-saghyz plants not to supply them with water while they are at rest.

The leaves were cut down with a sythe. A machine can also be applied for that purpose, but then, on account of the uneveness of the ground, the leaves are cut irregularly.

The operation was done when the upper parts of the plants turned yellow, which was taken as a sign of their going to fall into the dormant condition. In the district of Turkestan this period for two-year-old plants of tau-saghyz sets in by the end of July.

One or two days after the mowing of their leaves (never later) the plants received their first supply of water and the soil was loosened by hand. The plantation had also been watered, cultivated and hoed 10 days before the removal of leaves. In general it is essential before cutting away the leaves in two-year-old tau-saghyz plants to supply them with water 6 or 7 times, each time treating the soil adequately.

Seven days after first watering had followed the removal of leaves, the plants were again given water. After another 10 days they received water once more. A fortnight later water was supplied for the fourth time and after another fortnight, for the fifth time. In all, 12 waterings are necessary in the case of two-year-old tau-saghyz plants: 7 are made before the removal of leaves and 5 after. Each time the soil must be cultivated and loosened by manual implement.

In the third year of growth when the plants had come into fruit the plantation was treated in the normal manner, i. e. watered thrice previous to gathering the seed, each time with subsequent treatment of interrows. At the time of harvesting an additional watering is desirable. This time every other furrow must be watered. Otherwise the soil, owing to excessive moisture, would be rendered too dense by the harvesters.

On account of the agrotechnical measures referred to above, the plants of tau-saghyz escaped dormancy. The experimental plants went on growing at the expense of newly formed young leaves and this had a favourable effect upon the increase of root mass and the production of seeds (Tables 1 and 2).

So the highest yield of pure seed was obtained from the first lot of plants. They gave 87 kg per hectare more than did the controls. Their multiplication ratio

Table 1

Experimental lots	Yield of raw seeds with reference to cultivated area		Yield of seed in kg per hectare	
	Area	Yield in	Yield of raw seed	Yield of pure seed
1	0.50	153	306	102
2	0.56	134	240	80
3	0.51	23	45	15

Table 2

Experimental lots	Area under experiment in ha	Number of plants in thousands per ha	Yield of raw root in centners per ha	Average weight of one root in g
1	0.50	533	112	21
2	0.56	503	70.4	14
3	0.51	488	58.5	12

was 1 to 7, whereas in practice under ordinary conditions of cultivation the multiplication ratio of three-year-old tau-saghyz plants is usually 1 to 1.

From Table 2 it may be seen that the yield of root per hectare was by 53.5 centners greater in the first lot than in the control lot. It will be obvious that the elimination of summer dormancy in tau-saghyz plants very considerably increases their yield of both root and seed. The plants thus treated can be harvested after three years of growth, and there is no need to cultivate them for 5 to 7 years, as is the common practice to-day.

Received
4. X. 1942.

REFERENCES

* В. П. Малеев, Теоретич. основы акклиматизации (1933). [2] В. В. Щеглова, Период покоя у растений как признак для селекционного отбора. Селекция каучуконосных растений, сборник работ № 1 (1937). [3] Н. П. Кренке, Теория циклич. старения и омоложения растений (1941). [4] Т. Д. Лысенко, Теоретич. основы яровизации растений (1937). [5] Haberlandt, Beitr. allg. Bot., 2 (1922).

Comptes Rendus (Doklady) de l'Académie des Sciences de l'URSS
1943. Volume XXXVIII, № 2—3

GENERAL PATHOLOGY

EXPERIMENTAL SPRING-SUMMER TICK ENCEPHALITIS IN BIRDS

By S. P. ALFEEVA

(Communicated by E. N. Pavlovsky, Member of the Academy, 24.VIII.1942)

As a result of his investigation of the reservoirs of the virus of spring-summer tick encephalitis E. N. Pavlovsky has been brought to the assumption that birds inhabiting the tayga, when attacked by ticks, carriers of the encephalitis virus, may alongside of rodents serve as a reservoir of this virus (1).

Proceeding along the same line, I. A. Moskvin infected various species of birds, viz. *Loxia loxia*, *Acanthis flammea*, *Pyrrhula pyrrhula*, *Emberiza citronella*, *Chloris chloris*, *Passer domesticus*, with the virus of sping-summer encephalitis.

A number of species were found to be susceptible to the virus of the said disease which may assume either a manifest or latent form(2). The author used for the present work the same birds which had served to I. A. Moskvin for testing their susceptibility to the sping-summer encephalitis.

The fact that the same individuals were tested both for their susceptibility to tick encephalitis and for their ability to transmit the said infection to healthy animals (by inoculating them with an emulsion prepared from the cerebrum of the former) lays some limitation upon the scope of the pathologo-histological examination.

This does not, however, impair the work materially, since the emulsion is usually prepared of the great hemispheres of the cerebrum which are but slightly affected by the tick encephalitis.

The most severely affected parts of the cerebrum, viz. thalamus opticus, myelencephalon, pons Varolli, medulla oblongata, spinal cord, were subjected to histological examination.

The morphological alterations due to virus diseases of the neurotropic type consist in a primary affection of the ganglion cells, accompanied by a secondary inflammatory reaction. To each virus there corresponds a typical affection of some definite system of nerve-cells (see Doynikov, 1940).

The object of the present work was to bring out the morphological alterations that take place in the organs of birds experimentally infected with tick encephalitis.

A 10% emulsion prepared of the brain of a man who had perished from spring-summer encephalitis, was, after being passed through white rats, inoculated intracerebrally to the following birds: *Loxia loxia*, *Acanthis flammea*, *Pyrrhula pyrrhula*, *Emberiza citronella*, *Chloris chloris*, *Passer domesticus*, *Colocus monedula*, *Gallus* and *Parus caeruleus*. The last three species proved insusceptible to the virus of tick encephalitis.

The susceptibility of a given bird to the tick encephalitis was evaluated either by the symptoms of paralysis or paresis, in the case of a manifest form of the disease, or from the capacity to provoke encephalitis in a white rat when intracerebrally inoculated with an emulsion prepared of the cerebrum of the infected bird, in the case the form was a latent one.

The tested birds (57 in all) were divided into three lots according to the degree of the manifestation of the disease.

I, birds displaying phenomena of paresis or paralysis of legs, wings or head. Healthy birds or white rats intracerebrally given an emulsion prepared with the brain of diseased birds became infected with encephalitis.

II, birds in which we failed to observe either paresis or paralysis during their lifetime, but an emulsion of the brain of which when introduced intracerebrally produced in white rats infection with encephalitis.

III, birds which showed neither manifest nor latent form of encephalitis, irrespective of the fact whether they belonged to the susceptible or to the insusceptible group.

As control served eleven birds of the above-listed species; 6 of them perished of encephalitis and 5 were killed with ether.

The material was fixed with Zenker-formol, immersed in celloidine; sections were stained with haemotoxyline-eosin, eosin-azure, cresyl-violet, thionin, according to van-Gisson or to Malory. Aside from the trunk of the brain, medulla oblonga and spinal cord of the birds, there were also examined their hearts, lungs, livers, spleens and kidneys.

Microscopic examination has shown that the most severely affected is the central nervous system of the birds belonging to the first lot. Alterations were mostly observed in the thalamus opticus, myelencephalon, in the anterior horns of the upper dorsal or sacral segments of the spinal cord. The alterations may assume the form of shrivelling and darkening of definite groups of ganglion cells (observed in *Loxia loxia* No. 281, *Acanthis flammea* No. 289) or of swelling of ganglion cells, which may increase twice or thrice, of chromatolysis of the ganglion cells (e. g. in the anterior horns of the spinal cord of *Acanthis flammea*). Within the region of altered ganglion cells there is observed an increase in the number of glia elements; the diversity of cellular forms is sometimes diffuse in a definite part of the brain, sometimes this increase is perivascular or in the shape of small foci, while the ganglion cells remain unaltered. At a later date (10 days upon inoculation, second lot, *Pyrrhula pyrrhula* No. 291) the gliae display alterations in the form of proliferation and thickening. Alterations of the same kind, though less pronounced, were observed in some of the birds of the second lot. None of the birds belonging to the third lot showed alterations on the part of ganglion cells or gliae.

The examination of the internal organs of the birds revealed invariably a more or less pronounced hyperaemia: in the first lot haemorrhages were somewhat more frequent then in the rest. Infiltrations in the liver have been observed in 6 birds of the second and third lot; in the latter the increase of cellular elements in the glomeruli of the kidney was also more frequent than in other lots.

Microscopical examination of organs of the birds which had been found susceptible to the virus of tick encephalitis showed that the cells of the thalamus opticus, myelencephalon, of the anterior horns of the spinal cord had been the more affected, the sharper pronounced are the phenomena of paralysis. At the beginning the alterations of the ganglion cells were of regressive character; at later dates the glia changed progressively, which could be observed in birds of the second lot.

Because of the cadaveric changes, the cerebrum of birds that had perished could be used neither for preparation of emulsion, nor for microscopic examination.

The classification of the birds after the characters pointed out above as typical of each of the experimental lots was therefore a rather arbitrary one.

The method of inoculation to healthy animals of an emulsion prepared from the brain of birds affected with tick spring-summer encephalitis was of interest,

for it made it possible to discriminate between the virus encephalitis and the aseptic encephalitis which cannot usually be transmitted by passage; it permits, moreover, to bring out such forms of encephalitis which are accompanied with no phenomena of paresis or paralysis.

Conclusions

The morphological manifestations of tick encephalitis in birds consist in focal affections of definite systems of ganglion cells and of the surrounding glia. According to their localization (thalamus opticus, myelencephalon, anterior horns of the spinal cord), the foci correspond to the alterations taking place in the brain of man in the case of tick encephalitis and can be accounted for neither by mechanical irritation, nor by narcosis and fixation.

The alterations observed in the nerve cells are the more conspicuous, the more severe the phenomena of paralysis. In case the disease proceeded in a latent form, the alterations of the glia are mostly of proliferative character.

Department of General Biology and Parasitology.
S. M. Kirov Military Medical Academy.

Received
23. IX. 1942.

REFERENCES

[1] E. N. Pavlovsky, C. R. Acad. Sci. URSS, XXVIII, No. 2 (1940). [2] I. A. Moskvin, ibid., XXVIII, No. 2 (1940).

Comptes Rendus (Doklady) de l'Académie des Sciences de l'URSS
1943. Volume XXXVIII, № 2—3

PARASITOLOGY

LENGTH OF SURVIVAL UNDER WATER OF VARIOUS STAGES AND SPECIES OF TICKS, TRANSMITTERS OF PARASITIC ENCEPHALITIS IN THE MARITIME PROVINCE, FAR EAST OF THE USSR

By N. GRUZDEVA

(Communicated by E. N. Pavlovsky, Member of the Academy, 28.VIII. 1942)

Experiments involving the submergence of ticks, transmitters of the mite encephalitis, as suggested by E. N. Pavlovsky, have been planned with the aim of determining the length of survival under water of ticks at different phases of metamorphosis. The problem was of practical interest, since overflooding is likely to influence the possibility and terms of metamorphosis of ticks at foci of mite encephalitis.

The showers and floods that are of rather frequent occurrence in the Maritime province may certainly inhibit, if not check altogether, the development of separate phases of the mites; the less resistant among them may possibly be exterminated. This assumption is supported by the data obtained in 1936 by Springholz-Schmidt who submerged egg-laying females and eggs of *Dermacentor silvarum*; during these experiments the females were found to perish within the first days; considerable part of the eggs perished as well, and the rate of development of those that had survived was found to be slowed down considerably. The same phenomenon of delayed embryonic development and partial death of submerged eggs was reported by Olenev in 1941 for *Ixodes persulcatus* as a result of the experiments carried out in his laboratory in Leningrad.

Our experiments were carried on in the Suputinsk reserve; larvae, nymphae and imagoes of *Ixodes persulcatus*, *Haemaphysalis japonica* and *Dermacentor silvarum* were submerged mostly in a creek, but occasionally under laboratory conditions as well, at different months; from the data tabulated below it may be seen that the length of survival of the ticks at the same phases of metamorphosis varies according to season (Table 1).

The differences in the response of the ticks to submergence can be accounted for by their organism being less resistant to unfavourable factors in the active state, when all the vital processes are most intense, while it is more resistant in the inactive condition.

In fact, the ticks were found to be the least resistant at the beginning of August; in the second half of this month when their activity has already been somewhat abased by the rainy period and a general drop in the temperature, the period of their survival under water was found to have increased by 1—2 days.

The highest resistivity to submergence was shown by the ticks in September and especially in October, when the intensity of their vital processes had declined and the ticks made themselves ready to hibernation. Those of them which had underwent in October freezing under water (at laboratory conditions) were found upon thawing able to survive a rather prolonged submergence.

Table 1

Length of Survival under Water of Starving Ticks at Various Metamorphosis Phases as Related to Term and Duration of Submergence in the Course of Season

Date	Species and metamorphosis phase	Number of ticks	Number of ticks perished after beginning of submergence, in days																
			1	2	3	4	5	6	7	8	9	10	11	12	13	14	15	17	23
26 VI 1941	Imago of *Ixodes persulcatus* (in a creek)	100	0	0	4	33	14	?	30	16	?	3	—	—	—	—	—	—	—
	Imago of *Haemaphysalis concinna* (in a creek)	50	0	0	6	2	1	6	5	9	?	10	2	?	—	?	4*	—	—
5 VIII	Larvae of *Ixodes persulcatus* (in a creek)	50	?	40	5	0	1	—	—	—	—	—	—	—	—	—	—	—	—
	Do	50	?	34	10	0	3	—	—	—	—	—	—	—	—	—	—	—	—
	»	50	14	25	7	3	1	—	—	—	—	—	—	—	—	—	—	—	—
	Larvae of *Dermacentor silvarum* (in a creek)	50	?	35	12	1	—	—	—	—	—	—	—	—	—	—	—	—	—
	Do	50	43	7	—	—	—	—	—	—	—	—	—	—	—	—	—	—	—
	»	50	40	8	2	—	—	—	—	—	—	—	—	—	—	—	—	—	—
	Nymphae of *Dermacentor silvarum*	50	7	23	9	0	—	—	—	—	—	—	—	—	—	—	—	—	—
	Do	50	?	34	6	1	—	—	—	—	—	—	—	—	—	—	—	—	—
15 VIII	Larvae of *Ixodes persulcatus* (in a creek)	50	5	9	8	9	14	3	2	—	—	—	—	—	—	—	—	—	—
	Do	50	3	5	14	19	5	4	—	—	—	—	—	—	—	—	—	—	—
	»	50	0	5	11	21	4	5	4	—	—	—	—	—	—	—	—	—	—
	Larvae of *Dermacentor silvarum*	50	6	10	23	10	1	—	—	—	—	—	—	—	—	—	—	—	—
	Do	50	9	20	16	4	1	—	—	—	—	—	—	—	—	—	—	—	—
	»	50	4	24	18	4	—	—	—	—	—	—	—	—	—	—	—	—	—
	Nymphae of *Dermacentor silvarum*	25	0	2	3	6	9	4	1	—	—	—	—	—	—	—	—	—	—
	Do	25	0	4	5	9	7	—	—	—	—	—	—	—	—	—	—	—	—
	Nymphae of *Ixodes persulcatus* (in a creek)	25	0	2	1	1	0	1	0	4	—	—	—	—	—	—	—	—	—
15 IX	Larvae of *Haemaphysalis japonica* (in a creek)	50	0	0	0	0	1	0	11	6	—	—	—	—	—	—	—	—	—
18 IX	Do (under laboratory conditions)	50	7	0	0	43	—	—	—	—	—	—	—	—	—	—	—	—	—
	Nymphae of *Haemaphysalis japonica* (in a creek)	50	0	0	0	0	0	0	0	0	—	—	—	—	—	—	—	—	—
	Do (under laboratory conditions)	50	0	0	?	50	—	—	—	—	—	—	—	—	—	—	—	—	—
	Nymphae of *Ixodes persulcatus* (in a creek)	50	0	0	0	0	0	0	0	0	—	—	—	—	—	—	—	—	—
	Do (under laboratory conditions)	50	0	0	8	40	2	—	—	—	—	—	—	—	—	—	—	—	—
14 X	Larvae of *Ixodes persulcatus* (under laboratory conditions)	50	0	0	0	0	0	0	9	0	40	1	0	—	—	—	—	—	—
22 X	Do	50	0	0	0	0	0	0	0	0	0	0	0	?**	?	?	12	26	12
	Adult *Ixodes persulcatus* (under laboratory conditions)	12	0	0	0	0	0	0	0	0	0	0	0	—	—	—	—	—	—
	Adult *Haemaphysalis japonica* (under laboratory conditions)	10	0	0	0	0	0	0	0	0	0	0	0	—	0	0	—	—	—
	Adult *Dermacentor silvarum* (under laboratory conditions)	5	0	0	0	—	—	—	—	—	—	—	—	—	—	—	—	—	—

*Five ticks survived.

**Were frozen into ice during 24 hours.

The above interpretation of the varying length of survival of ticks at the period, when they do not feed, seems to be corroborated by experiments involving the submergence of starving larvae and of nymphae in September in a creek and under laboratory conditions. The intensity of vital processes is increased by the higher temperature of laboratory water as compared to that of the creek (the maxima being 16—18° C and 9—9.5° C, respectively). This is the reason of the lower resistance of the ticks in inundation. Among all phases the most sensitive to submergence proved the starving larvae, in particular those of the species *Dermacentor silvarum*, whereas the most resistant were found to be the adult-ticks (Table 2).

Table 2

Time of Submergence of Fed Ticks and Terms of Their Subsequent Moult

Species and metamorphosis phase	Time of submergence	Date of submergence	Beginning of moult after	Note
Larvae of *Ix. persulcatus* (in a creek)	3 24-hour days	1st half of August	37 days	
Do	3 »	Do	34 »	
Nymphae of *Ix. persulcatus*	2 »	»	40 »	Flight of ichneumons
Do	3 »	»	40 »	Do
»	2 »	2nd half of July	37 »	
»	4 »	Do	38 »	
»	11 »	»	45	
Nymphae of *D. silvarum*	2 »	August	18 »	Flight of ichneumons
Do	4	July	31 »	Part of the nymphae failed to moult in 1941
»	6 »	»	32 »	
Larvae of *D. silvarum*	3 »	August	7 »	
Do	9 »	»	9 »	
»	5 »	»	11 »	
Nymphae of *D. silvarum*	3 »	»	23 »	
Do	3 »	»	23 »	

From the data on submergence of fed larvae and nymphae contained in Table 2 it is evident that these stages go on moulting after submergence; the beginning of the moult, however, is somewhat delayed according to the duration of submergence. The delay was rather considerable in case the experiment lasted eleven 24-hour days, the loss of ticks being as high as 79%. A two- or three-day submergence of the fed ticks had a smaller effect upon the terms of moulting, the per cent of loss reaching an average of 15.

It is of interest to note that a two- or three-day submergence has no effect upon the ichneumon flies, parasitic of the tick; the flight of the former was observed upon the submergence of fed nymphae in three cases.

Laboratory for Parasitology
of the Altitude Tayga Station.
Academy of Sciences of the USSR.

Received
28. VIII. 1942.

Prix $ 0.50